



## Structure–activity relationship study of nitrosopyrimidines acting as antifungal agents

Monica Olivella<sup>a</sup>, Antonio Marchal<sup>b</sup>, Manuel Noguera<sup>b</sup>, Adolfo Sánchez<sup>b</sup>, Manuel Melguizo<sup>b</sup>, Marcela Raimondi<sup>c,d</sup>, Susana Zacchino<sup>c</sup>, Fernando Giannini<sup>a</sup>, Justo Cobo<sup>b,\*</sup>, Ricardo D. Enriz<sup>a,e,\*</sup>

<sup>a</sup> Departamento de Química, Facultad de Química, Bioquímica y Farmacia, Universidad Nacional de San Luis, Chacabuco 915, 5700 San Luis, Argentina

<sup>b</sup> Departamento de Química Inorgánica y Orgánica, Universidad de Jaén, 23071 Jaén, Spain

<sup>c</sup> Farmacognosia, Facultad de Ciencias Bioquímicas y Farmacéuticas, Universidad Nacional de Rosario, Suipacha 531, 2000 Rosario, Argentina

<sup>d</sup> Microbiología, Facultad de Medicina, Universidad Nacional de Rosario, Santa Fe 3100, 2000 Rosario, Argentina

<sup>e</sup> IMIBIO-SL (CONICET), Chacabuco 915, 5700 San Luis, Argentina

### ARTICLE INFO

#### Article history:

Received 6 June 2012

Revised 8 August 2012

Accepted 16 August 2012

Available online 31 August 2012

#### Keywords:

Nitrosopyrimidines

Antifungal compounds

Synthesis

Structure–activity relationships

Conformational study

### ABSTRACT

The design, synthesis, in vitro evaluation, and conformational study of nitrosopyrimidine derivatives acting as antifungal agents are reported. Different compounds structurally related with 4,6-bis(alkyl or arylamino)-5-nitrosopyrimidines were evaluated. Some of these nitrosopyrimidines have displayed a significant antifungal activity against human pathogenic strains. In this paper, we report a new group of nitrosopyrimidines acting as antifungal agents. Among them, compounds **2a**, **2b** and **15**, the latter obtained from a molecular modeling study, exhibited antifungal activity against *Candida albicans*, *Candida tropicalis* and *Cryptococcus neoformans*. We have performed a conformational and electronic analysis on these compounds by using quantum mechanics calculations in conjunction with Molecular Electrostatic Potentials (MEP) obtained from B3LYP/6–31G(d) calculations. Our experimental and theoretical results have led us to identify a topographical template which may provide a guide for the design of new nitrosopyrimidines with antifungal effects.

© 2012 Elsevier Ltd. All rights reserved.

### 1. Introduction

Fungal infections have continued to be a major medical problem during the past two decades especially involving immunocompromised patients.<sup>1,3</sup> Although it appears to be many drugs for the treatment of systemic and superficial mycoses, there are in fact only a limited number of efficacious antifungal drugs.<sup>2</sup> Azoles that inhibit ergosterol biosynthesis and polyenes that bind to mature membrane sterols have been the mainstays of antifungal therapy for more than two decades.<sup>4,5</sup> However, the emergence of fluconazole resistance among different pathogenic strains and the high toxicity of amphotericin B,<sup>6,7</sup> have led to the search for new antifungal agents.<sup>8</sup> Although combination therapy has emerged as a good alternative to overcome these disadvantages,<sup>9,10</sup> there is a real need for a next generation of safer and more potent antifungal agents.<sup>2</sup>

In the course of our ongoing screening program for new antifungal compounds, we have previously reported the antifungal activity of peptide compounds<sup>11–17</sup> as well as of different molecules obtained from natural<sup>18–21</sup> and synthetic<sup>22–31</sup> sources.

Among them, a series of 4-aryl- or 4-alkyl-*N*-arylamino-1-butenes (homoallylamines) and related tetrahydroquinolines and quinolines displayed a range of antifungal properties against dermatophytes, which are responsible of most dermatomycoses in humans.<sup>22</sup> Afterwards, we extended our study by introducing a new series of 4-*N*-arylamino-1-butenes containing the pyridinyl or quinolinyl moieties at C4 and other structurally related compounds.<sup>24</sup> The structure–activity relationship (SAR) analysis indicated that the presence of two aromatic rings and a particular length for the connecting chain are operative for the homoallylamine derivatives.<sup>28</sup>

Although the previously reported homoallylamines displayed an interesting antifungal activity, unfortunately their effects were limited to dermatophytes and they did not show any significant activity against other opportunistic clinical relevant fungi. It is well known that many fungal infections are caused by opportunistic pathogens that may be endogenous or acquired from the environment. Patients with significant immunosuppression frequently develop candidiasis or cryptococcosis.

Candidiasis has shown to be the fourth most common nosocomial blood stream infection, *Candida albicans* representing more than 60% of all isolates from clinical infections.<sup>32</sup> Among the non-*albicans* *Candida* species, *Candida tropicalis* showed to be the most isolated species (20%) in Latin American countries between

\* Corresponding authors. Tel.: +34 953212695 (J.C.); tel.: +54 2664 424689x153 (R.D.E.).

E-mail addresses: [jcobo@ujaen.es](mailto:jcobo@ujaen.es) (J. Cobo), [denriz@unsl.edu.ar](mailto:denriz@unsl.edu.ar) (R.D. Enriz).

2001 and 2004. *Cryptococcosis*, caused by the encapsulated yeast *Cryptococcus neoformans*, has been the leading cause of fungal mortality among immune-suppressed patients.<sup>6</sup> This organism has predilection for the central nervous system and leads to severe, life-threatening meningitis.

Invasive aspergillosis is a rapidly progressive, often fatal infection that occurs in patients who are severely immunosuppressed, including those who are profoundly neutropenic, those who have received bone marrow or solid organ transplants, and patients with advanced AIDS or chronic granulomatous disease.<sup>33</sup> The majority of human illness is caused by *Aspergillus fumigatus* and *Aspergillus niger* and, less frequently, by *Aspergillus flavus*.

Considering that homoalylamines previously reported displayed two aromatic rings, we start our study using compounds possessing such structural characteristics. In addition taking advantage of our previous experience in the synthesis of aminopyrimidines bearing the same structural characteristics,<sup>34</sup> we decided to look for new compounds structurally related to the homoalylamines previously reported. In addition, we have recently reported that the introduction of a nitroso group on C5 of a pyrimidine nucleus highly activates it towards nucleophilic substitution. This enables the easy and selective displacement of methoxy groups in 2-amino-4,6-dimethoxy-5-nitrosopyrimidine by a large series of amines under mild conditions, allowing efficient, time-saving, one-pot preparations of symmetrical and non-symmetrical 2,4,6-tris(alkylamino)-5-nitrosopyrimidines, which are useful as intermediates in common synthetic routes to heterobicyclic systems of great biological interest.<sup>34a</sup>

In this study we have determined the antifungal activity of nitrosopyrimidine derivatives against a panel of clinically important fungi. With these results we have performed a structure-activity relationship (SAR) study in order to determine the minimum structural requirements for these compounds to produce the antifungal effect. We also discuss here a possible pharmacophoric model for these compounds and the stereoelectronic requirements necessary to elicit the activity. In addition, a molecular modeling study supported by quantum mechanic calculations allowed us to design, synthesize and test new active compounds of this series.

## 2. Results and discussion

### 2.1. Chemistry

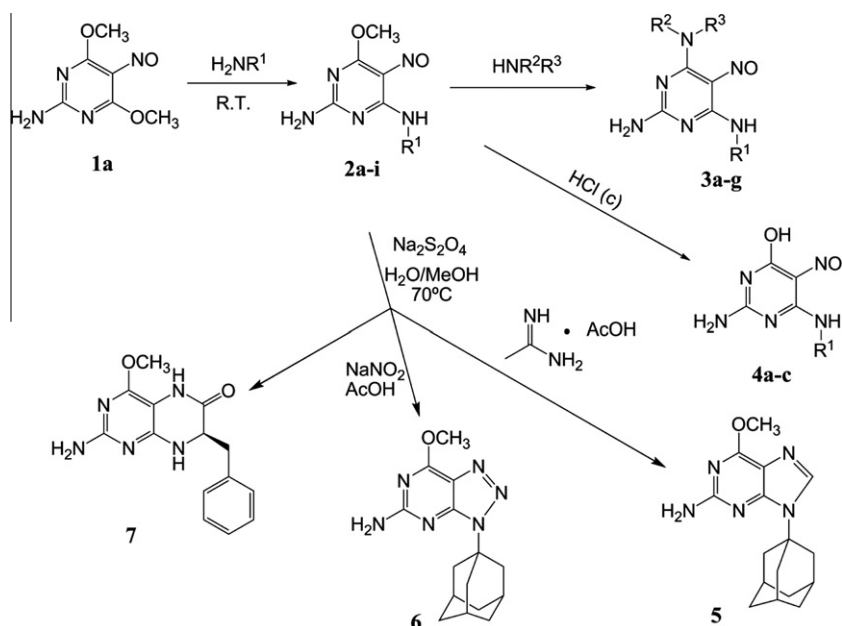
We have already reported the synthesis of a family of  $N^4$ -substituted 2,4-diamino-6-methoxy-5-nitrosopyrimidines **2** by selective monoaminolysis of **1a**,<sup>34a-c</sup> which was prepared through the introduction of a 5-nitroso group into the commercial 2-amino-4,6-dimethoxypyrimidine (see Scheme 1 and Table 1). A second aminolysis with a different amino compound permitted us the preparation of a set of highly functionalized  $N^4, N^6$ -disubstituted 2,4,6-triamino-5-nitrosopyrimidines **3** (see Scheme 1 and Table 1). We have also isolated in some of these reactions the hydrolysis products such as several  $N^6$ -substituted 2,6-diamino-5-nitrosopyrimidin-4(3H)ones **4** (see Scheme 1).

All of these ortho-aminonitrosopyrimidines, such as **2**, **3** or **4**, are very useful as synthetic intermediates to purine or pteridine analogues, which, by reduction of the nitroso to an amino group and further cyclocondensation can afford easily this kind of compounds; for example the cyclocondensation with formamidinium acetate or with sodium nitrite in acid media, leads to the corresponding purine, or azapurine analogues, **5** or **6** respectively if starting from **2c** (Scheme 1). If starting from **2i**, the reduction of the nitroso group is followed by an intramolecular cyclization through an ester group rendering the pteridine analogue **7** as showed in Scheme 1.

In order to increase the structural diversity and also to test the influence of changing different groups, or the size of the fused ring to pyrimidine, we have prepared the pteridine analogues **9a, b** and **10** (Scheme 2). So, changing the methoxy group at **1a** by a bulkier group, such as cyclohexylmethylenoxy, by transalkoxylation we have synthesized compound **1b**, which, by further substitution with different aminoesters yielded **8a, b**, which were used, in a similar procedure to that employed to get the pteridine **7**, for the preparation of analogues **9a, b**.

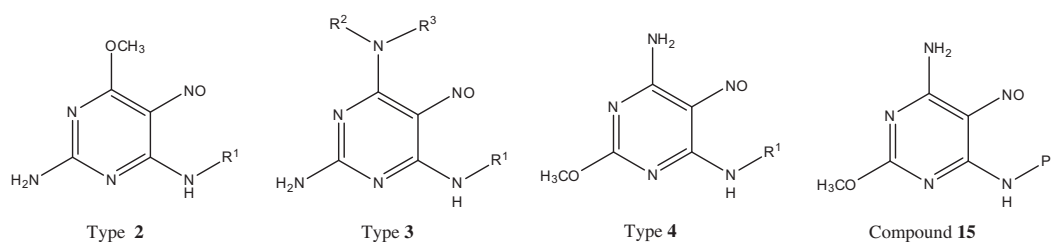
Compound **10** is a pteridine analogue, prepared from **2h** by a similar procedure, in which instead of a six membered ring it has a seven membered ring fused to pyrimidine.

We have modified the free amino at C-2 of the pyrimidine ring as well; thus, different derivatives related to **2** such as **11a, b, c**,



**Scheme 1.** Synthetic sequence for the preparation of fused pyrimidines via nitrosation-aminolysis-reduction-cyclization from methoxypyrimidines.

**Table 1**  
Structural features of compounds **2**, **3** and **4** and **15**



Compd type 2		Compd type 3			Compd type 4
R <sup>1</sup>		R <sup>1</sup>	R <sup>2</sup>	R <sup>3</sup>	R <sup>1</sup>
<b>a</b>	(3-Cl)C <sub>6</sub> H <sub>4</sub>	(3-Cl)C <sub>6</sub> H <sub>4</sub>	<i>i</i> Pr	H	CH( <i>s</i> -Bu)CO <sub>2</sub> H
<b>b</b>	Bu	Bu	Ph	H	CH(CH <sub>2</sub> OH)CO <sub>2</sub> H
<b>c</b>	Ad	Bn	<i>i</i> Pr	H	Ad
<b>d</b>	(CH <sub>2</sub> ) <sub>2</sub> O(CH <sub>2</sub> ) <sub>2</sub> OH	Bn	CH <sub>3</sub>	H	
<b>e</b>	(CH <sub>2</sub> ) <sub>2</sub> -OH	Bn	Bn	H	
<b>f</b>	CH <sub>2</sub> CO <sub>2</sub> Et	(CH <sub>2</sub> ) <sub>2</sub> CO <sub>2</sub> Et	Ph	H	
<b>g</b>	CHCH <sub>3</sub> CO <sub>2</sub> Et	Cyclohexyl	-(CH <sub>2</sub> ) <sub>4</sub> -	-(CH <sub>2</sub> ) <sub>4</sub> -	
<b>h</b>	(CH <sub>2</sub> ) <sub>2</sub> CO <sub>2</sub> Et				
<b>i</b>	CHBnCO <sub>2</sub> Et				

were obtained (Scheme 3). These compounds possess an ethylene linker between amino and another potential hydrogen donor and/or acceptor group, such hydroxyl **11a** or acetoxy groups **11b,c**. These molecules were prepared by a similar procedure to that described above in Schemes 1 and 2; the modification of amino group at C-2 was done in a first step from 2-chloro-4,6-dimethoxy-pyrimidine I by nucleophilic substitution with  $\beta$ -aminoethanol.

Finally, we have prepared several 5-nitroso derivatives, such **12**, **13** and **14** with a 4-amino-2-methoxypyrimidine moiety, in which these two groups were exchanged respect to the previously synthesized compounds. So, we have firstly prepared the nitrosopyrimidine **1c**, isomer of **1a**, from the commercial 4-amino-2,6-dimethoxypyrimidine using the reported nitrosation procedure,<sup>34b</sup> to be used as precursor for the preparation of compound **12**, related to the set of compounds **2** (Scheme 4).

As a last structural change, we included the lactamic form in the pyrimidine ring instead of the heteroaromatic one, so we performed a benzylation reaction on 4-amino-2-methoxypyrimidin-4(3H)one **III** to get the corresponding N-benzylated derivative **IV**, that is obtained along with its O-benzylated heteroaromatic isomer **V**. Once those isomeric derivatives were separated, they were independently subjected to our nitrosation procedure (see Scheme 5) to get their 5-nitroso derivatives, **13** and **14** respectively.<sup>34a</sup>

Finally, after performing the antifungal assays of the above compounds, and as a direct consequence of the results obtained in our molecular modeling study (see Section 2.3), we decided to synthesize compound **15** (Table 1) as described in Scheme 4 using aniline in the selective monoamination of **1c**.

In summary compounds **9a–b**, **10**, **11a–c**, **12**, **13** and **15** are reported here for the first time.

## 2.2. Antifungal activity and structure–activity relationships

We tested, at first, the antifungal effects of the 23 previously reported compounds: **1a**, **2a–i**, **3a–g**, **4a–c**, **5**, **6**, **7** and **14** against a panel of clinically important fungi such as the yeasts *C. albicans*, *C. tropicalis*, *C. neoformans*, the hialohyphomycetes *Aspergillus flavus*, *A. fumigatus* and *A. niger*, and the dermatophytes *Microsporum gypseum*, *Trichophyton rubrum* and *Trichophyton mentagrophytes*.

Compounds **2a**, **2b**, **5** and **14** displayed moderate to low (although selective) antifungal activities (MICs between 31.2 to >250  $\mu$ g/mL) against the yeasts *C. albicans*, *C. tropicalis*, *C. neoformans* and some of them against dermatophytes, being fungicide rather than fungistatic. In contrast, *Aspergillus* spp. did not show susceptibility to nitrosopyrimidines and related compounds (Table 2).

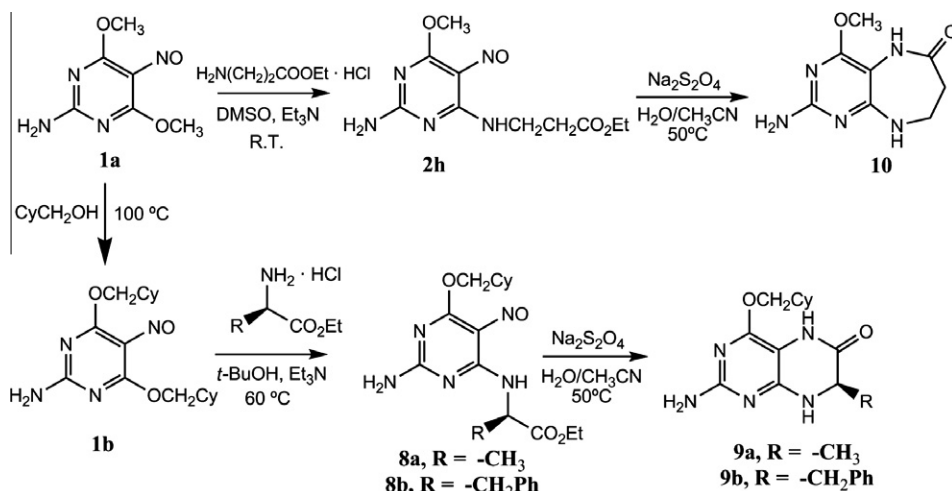
However, it is important to take into account that these MIC values refer to the minimum concentration necessary to inhibit 100% of the fungal growth. If, as recommended by standardized documents,<sup>35,36</sup> less stringent end-points such as MIC<sub>50</sub> (the minimum concentration of compounds that inhibit 50% of growth, respectively) are determined, lower minimum inhibitory concentrations for each compound would be obtained. In addition, the application of less stringent end-points many times provide a better correlation with other measurements of antifungal activity.<sup>22,23</sup>

Compounds **2a**, **2b**, **5** and **14** were tested again, against *C. albicans* ATCC 10231 and *C. neoformans* ATCC 32264 by using a similar microplate design than that used for determining MIC<sub>100</sub>. The aim was determine the inhibition percentages displayed by each compound at the different concentrations, which were calculated with the aid of a microplate reader, as explained in material and methods. These results are presented in Table 3.

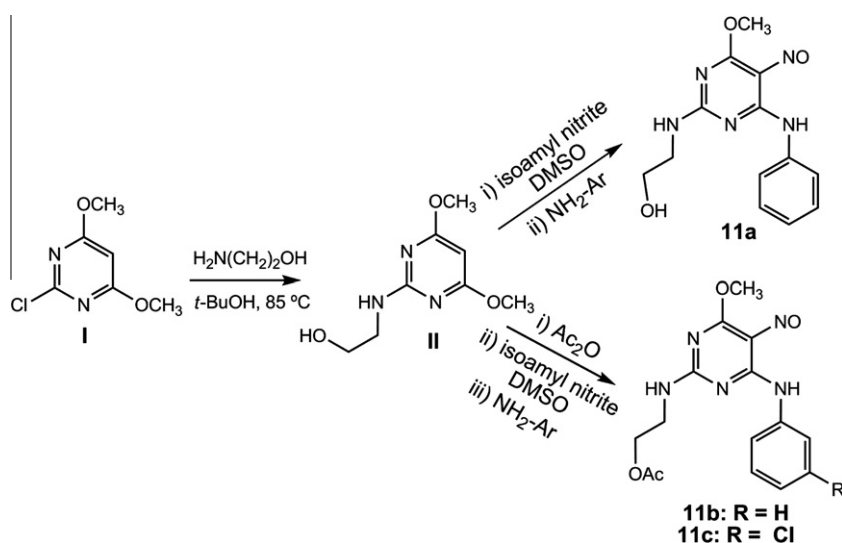
Compound **5** displayed just a moderated antifungal activity (MIC<sub>50</sub> = 31.25–62.5  $\mu$ g/mL), which is in contrast with compounds **2a**, **2b** and **14** which displayed higher antifungal activities with MIC<sub>50</sub> values ranging from 1.95 to 7.8  $\mu$ g/mL.

Since the toxicity of any potential antifungal agent is a critical aspect for its usefulness and limitations, the acute toxicity for compounds **2a**, **2b** and **14** were evaluated using a toxicity test on fishes which has been successfully used by our group with other antifungal compounds.<sup>20–37</sup> Our results indicated that compound **14** possessed a high acute toxicity. It displayed 100% of mortality at 1.6  $\mu$ g/mL and 0.8  $\mu$ g/mL at 24 and 48 h respectively (Table 1S in Supplementary material). In contrast, acute toxicities were not observed (0% mortality) with 38.4  $\mu$ g/mL of **2a** or 35  $\mu$ g/mL of **2b**, concentrations clearly higher than the antifungal ones for both compounds.

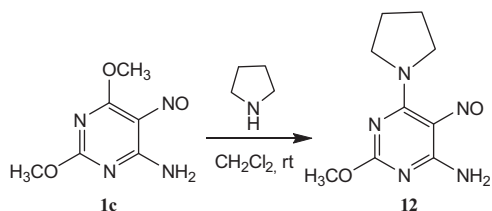
Nitrosopyrimidines and analogues reported in the previous section provided a considerable diversity of chemical structures and



**Scheme 2.** Preparation of new pteridine analogues from alkoxy-nitrosopyrimidines.



**Scheme 3.** Preparation of some  $N^2,N^4$ -disubstituted 2,4-diamino-5-nitrosopyrimidines.



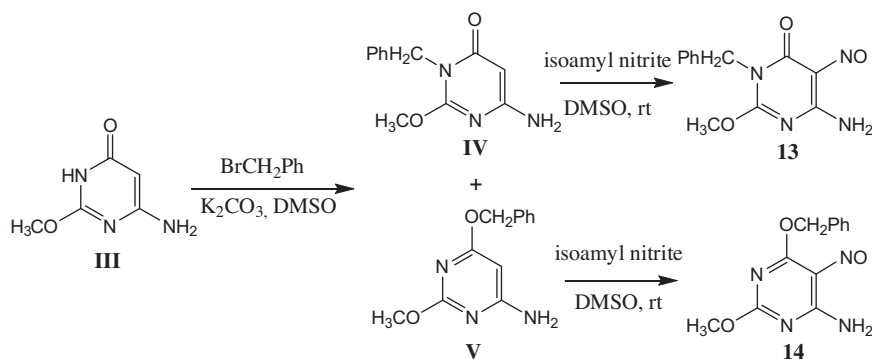
**Scheme 4.** Synthesis of 4-amino-2-methoxy-5-nitroso-6-(pyrrolidin-1-yl)pyrimidine **12**.

therefore, from the analysis of their structures and the antifungal activities displayed, some Structure–Activity Relationships can be extracted. This SAR analysis was performed considering the following structural changes:

- Different types of aromatic central rings
- Different substituents on the aromatic central ring
- Molecular flexibility
  - The active compounds **2a** and **2b** have the same aromatic central ring; in contrast compounds **5** and **14** possess different aromatic central rings. It should be noted that compound

**5** displayed only a moderate antifungal activity. The presence of a non-substituted amino group in type 2-compounds appears to be necessary to produce the antifungal activity. Type 3-compounds, possessing substituents of different size **3a**, **3b**, **3c**, **3d**, **3e** and **3f** were all inactive. These results suggest that the presence of donor or acceptor groups such as  $\text{NH}_2$  or  $\text{OCH}_3$  in the central ring might be necessary to produce the biological response. Compounds **3g** and **7** were also inactive giving an additional support to this hypothesis. In order to corroborate this assumption, we synthesized compounds **12** and **13** possessing different central rings. None of them displayed any antifungal activity supporting, at least in part, our assumption.

- Regarding the results shown in Table 2 it is evident that the presence of an aromatic central ring type **2** might be important for the antifungal activity; however it is not by itself enough to produce the biological response. The type of substituents on the central ring appears to play an important role in the antifungal effect. Replacement of hydrophobic groups by more polar systems at  $N^4$ -substituent gives inactive compounds. Compounds **2d–i**, and **4a,b** illustrate this situation very well. In contrast, the replacement of *m*-ClPhe



**Scheme 5.** Synthesis of lactamic 4-amino-3-benzyl-2-methoxypyrimidin-4(3H)one **13** along with its 4-O-benzyl heteroaromatic isomer **14** <sup>34a</sup>.

**Table 2**

Minimum inhibitory concentrations and Minimum Fungicide Concentration (MIC and MFC in  $\mu\text{g/mL}$ , showed as MIC/MFC). *Ca* (*C. albicans*), *Ct* (*C. tropicalis*), *Cn* (*C. neoformans*), *Afu* *A. fumigatus*, *Ani* (*A. niger*), *Mg* (*M. gypseum*), *Tr* (*T. rubrum*), *Tm* (*T. mentagrophytes*).

Compd	<i>Ca</i>	<i>Ct</i>	<i>Cn</i>	<i>Afl</i>	<i>Afu</i>	<i>Ani</i>	<i>Mg</i>	<i>Tr</i>	<i>Tm</i>
<b>1a,b</b>	i	i	i	i	i	i	i	i	i
<b>2a</b>	125/i	125/i	125/250	i	i	i	i	i	i
<b>2b</b>	62.5/250	62.5/250	125/250	i	i	i	i	250/i	250/i
<b>2c-i</b>	i	i	i	i	i	i	i	i	i
<b>3a-3g</b>	i	i	i	i	i	i	i	i	i
<b>4a-4c</b>	i	i	i	i	i	i	i	i	i
<b>5</b>	250/i	250/i	250/i	i	i	i	i	i	i
<b>6</b>	i	i	i	i	i	i	i	i	i
<b>7</b>	i	i	i	i	i	i	i	i	i
<b>8a,b</b>	i	i	i	i	i	i	i	i	i
<b>9a,b</b>	i	i	i	i	i	i	i	i	i
<b>10</b>	i	i	i	i	i	i	i	i	i
<b>11a,b,c</b>	i	i	i	i	i	i	i	i	i
<b>12</b>	i	i	i	i	i	i	i	i	i
<b>13</b>	i	i	i	i	i	i	i	i	i
<b>14</b>	31.2/62.5	31.2/62.5	62.5/125	i	i	i	62.5/62.5	125/125	125/125
<b>15</b>	31.2/31.2	31.2/31.2	15.6/62.5	i	i	i	62.5/62.5	125/250	125/250
<b>Amp</b>	0.98	0.98	0.25	0.49	0.49	0.49	0.12	0.06	0.06
<b>Terb</b>	0.98	1.95	0.49	0.98	0.98	1.96	0.04	0.01	0.03
<b>Ket</b>	0.98	0.49	0.25	0.12	0.49	0.25	0.06	0.03	0.03

Compound **15** is highlighted in grey because it was synthesized and tested in a second instance as the result of a computational design. See Section 2.3.

**Table 3**

Antifungal activity (inhibition %, and MIC<sub>50</sub> values) obtained for the most active compounds against *C. albicans*, *C. tropicalis* and *C. neoformans*.

Compound	Concentration in $\mu\text{g/ml}$							
	250	125	62.5	31.25	15.6	7.8	3.9	MIC <sub>50</sub>
<i>Candida albicans</i>								
<b>2a</b>	100	100	92.7 $\pm$ 0.3	91.8 $\pm$ 0.5	86.3 $\pm$ 0.4	80.3 $\pm$ 4.6	53.3 $\pm$ 0.0	3.9
<b>2b</b>	100	100	100	98.2 $\pm$ 0.9	86.2 $\pm$ 0.6	50.4 $\pm$ 4.1	20.0 $\pm$ 1.38	7.8
<b>5</b>	100	86.8 $\pm$ 1.8	43.4 $\pm$ 0.1	38.9 $\pm$ 4.3	34.3 $\pm$ 0.7	23.2 $\pm$ 2.1	29.3 $\pm$ 5.2	62.5
<b>14</b>	100	100	100	100	99.6 $\pm$ 1.4	56.9 $\pm$ 1.6	47.2 $\pm$ 2.7	7.8
<b>15</b>	100	100	100	100	98.1 $\pm$ 4.8	85.0 $\pm$ 3.0	4.7 $\pm$ 2.6	7.8
<b>Amp</b>								0.49
<i>Candida tropicalis</i>								
<b>2a</b>	100	100	87.9 $\pm$ 1.5	85.2 $\pm$ 1.2	75.2 $\pm$ 4.8	64.5 $\pm$ 2.9	48.8 $\pm$ 6.4	3.9
<b>2b</b>	100	100	100	93.2 $\pm$ 5.8	85.2 $\pm$ 1.8	57.7 $\pm$ 6.1	16.3 $\pm$ 5.9	7.8
<b>5</b>	100	81.2 $\pm$ 0.8	53.3 $\pm$ 6.6	47.3 $\pm$ 0.5	41.5 $\pm$ 3.9	34.5 $\pm$ 3.8	36.4 $\pm$ 6.4	62.5
<b>14</b>	100	100	100	100	96.7 $\pm$ 2.6	56.7 $\pm$ 2.6	19.7 $\pm$ 1.3	7.8
<b>15</b>	100	100	100	100	88.2 $\pm$ 8.9	87.2 $\pm$ 2.2	4.1 $\pm$ 2.9	7.8
<b>Amp</b>								0.49
<i>Cryptococcus neoformans</i>								
<b>2a</b>	100	100	83.7 $\pm$ 2.0	81.3 $\pm$ 4.8	80.6 $\pm$ 6.2	74.9 $\pm$ 8.9	53.2 $\pm$ 3.9	3.9
<b>2b</b>	100	100	85.5 $\pm$ 1.4	75.0 $\pm$ 8.6	63.1 $\pm$ 8.6	52.4 $\pm$ 1.3	11.3 $\pm$ 1.1	7.8
<b>5</b>	100	88.0 $\pm$ 2.9	51.1 $\pm$ 0.2	56.9 $\pm$ 4.9	39.2 $\pm$ 1.2	9.5 $\pm$ 1.9	0	31.25
<b>14</b>	100	100	100	88.1 $\pm$ 2.9	80.2 $\pm$ 3.2	78.1 $\pm$ 1.5	49.2 $\pm$ 4.1	3.9
<b>15</b>	100	100	100	100	100	91.2 $\pm$ 1.6	76.2 $\pm$ 1.9	1.95
<b>Amp</b>								0.98

of compound **2a** by butyl in compound **2b** was well tolerated, keeping the antifungal activity. It is interesting to note

that compound **2b** possesses just one aromatic ring. This is a striking difference with respect to the structural require-

ments previously reported for homoallylamines.<sup>22,24,28,29</sup> However, it appears that not any hydrophobic substituent is operative; note that the replacement of a butyl group of **2b** by adamantane in **2c** give an inactive compound. In order to evaluate if a similar behavior might be also observed for the  $N^d$ -substituents if a 2-amino group is modified, we synthesized compounds **11a,b,c**. Our results indicated that the presence of relatively polar  $N^d$ -substituents produces loss of activity (compare **2a** with **11c**). Compounds **11a** and **11b** give additional support to this observation.

- c) Compound **5**, possessing a conformationally constrained structure, displayed only a moderate antifungal activity; whereas compound **7** possessing a comparable restricted molecular flexibility was totally inactive. These results suggest that a relative molecular flexibility could be necessary in these compounds to produce the antifungal activity. To better understand such situation we synthesized and tested the conformationally restricted compounds **10**, **9a** and **9b**. None of these compounds displayed antifungal activity. It should be noted that the only structural difference between compounds **6** and **5** is the replacement of N by C. However, this apparently minor structural change produces the complete loss of activity for compound **6**.

It must be pointed out that all the above structural changes were carried out without taking into account the possible changes in the physicochemical properties introduced with each structural modification. None of the new nitrosopyrimidines synthesized (**9a**, **9b**, **10**, **11a–c**, **12** and **13**) displayed antifungal activity; they do not completely inhibit the growth of fungi even at high concentrations. Therefore, these results prompted us to develop a new nitrosopyrimidine structure but now using a more rational design based on theoretical calculations. Thus, in the next step of our study we decided to perform an exhaustive conformational and electronic study on the active compounds **2a**, **2b** and **5** in order to determine the stereoelectronic characteristics which could be useful to design new compounds possessing similar properties.

### 2.3. Conformational and electronic study of nitrosopyrimidines

In an attempt to explain the above experimental results as well as to find a new active compound, we conducted a computer-assisted conformational and electronic study on compounds **2a**, **2b** and **5**. The purpose was to obtain more precise information about how these compounds resemble each other in terms of the spatial orientations of the essential components to produce the biological response. Compound **2a** looks like a relatively simple conformational problem with three torsional angles ( $\Phi_1$ ,  $\Phi_2$  and  $\Phi_3$ , Fig. 1). In this compound the orientations of the ring systems are described by the dihedral angles  $\Phi_2$  and  $\Phi_3$ ; whereas the orientations of the nitroso group are described by the dihedral angle  $\Phi_1$ . Our calculations predicts that the torsional angle  $\Phi_1$  possesses only two possible quasi-planar conformations: one of them near to  $0^\circ$  which allows the formation of a hydrogen bond between the oxygen atom of nitroso group and the NH of the connecting chain; in contrast in the other conformer the oxygen atom of nitroso group is located in the opposite position giving values near to  $180^\circ$ . Compound **2a** has a numerable number of conformers on its Potential Energy Surface (PES) but, where does one form change to the other and how far from an energy minimum can the molecule stray away before ceasing to be in a conformation referred to as the energy minimum? It is clear, that information about local and global minima of a molecule such as compound **2a** is not enough. We need to have at least a good notion of the shape and also some indication about the dynamic behavior of the internal degrees of freedom of this molecule. Probably the most comprehensive computational

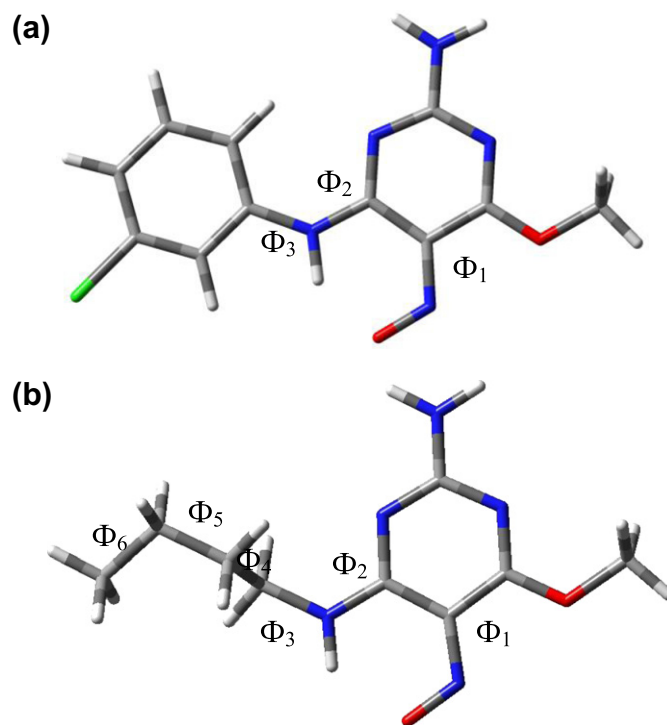


**Figure 1.** Spatial view of the lowest-energy conformations obtained for compounds **2a** (a) and **2b** (b). In these figures carbon atoms are marked with grey; chlorine with green; hydrogens with white; nitrogens with blue and oxygen with red. The different torsional angles are also shown in this figure.

method to answer the above questions is to find out how the local energy minima and the transition states are linked together, and this requires an exploration of the complete PESs. The PESs were calculated using a  $12 \times 12$  grid generated by rotating through  $\Phi_2$  and  $\Phi_3$  in  $30^\circ$  increments from  $-180$  to  $180^\circ$ . At each point a complete geometry optimization was performed with  $\Phi_2$  and  $\Phi_3$  frozen at their respective grid values. Thus, considering that  $\Phi_1$  might adopt two conformations, two different PESs were calculated for compound **2a** in which  $\Phi_1$  is located near to  $0^\circ$  and near to  $180^\circ$  (Fig. 2a and 2b, respectively).

The lowest-energy structures of compound **2a** are planar forms possessing a stabilizing hydrogen bond (see Fig. 1a). These conformers also can be seen in the contour and surface plots of fig. 2a as the minima centered at ( $\Phi_2$  and  $\Phi_3$ ) (0.0, 0.0, conformation 1) and its symmetry-related partner (0.0,  $180.0$ , conformation 2). The set of symmetry-related anti-coplanar structures (near to  $180$ ,  $180$  and  $180$ ,  $0$ , conformations 5 and 6, respectively) lies approximately 17 Kcal/mol above the preferred conformers. It is interesting to note that the interconversion between the two preferred forms requires about 3 kcal/mol indicating that this molecule possesses a high molecular flexibility in such spatial zone. In contrast, the conformational interconversion between conformer **1** with **4** requires about 22 Kcal/mol.

Figure 2b shows the PES obtained for compound **2a** scanning  $\Phi_2$  and  $\Phi_3$  when  $\Phi_1$  is located near to  $180^\circ$ . The four different low-energy conformers (conformations **3**, **4**, **7** and **8**) might be well appreciated in this surface. Note that the spatial positions obtained for the different conformers as well as their respective energy gaps displayed in Figure 2a and Table 4 are closely related but they are not exactly equal. This is an expected result considering that they were obtained from different levels of calculations.

It should be noted that these PESs were obtained from RHF calculations using a modest basis set (3-21G); therefore, in order to confirm that the molecular flexibility and the relative stability of

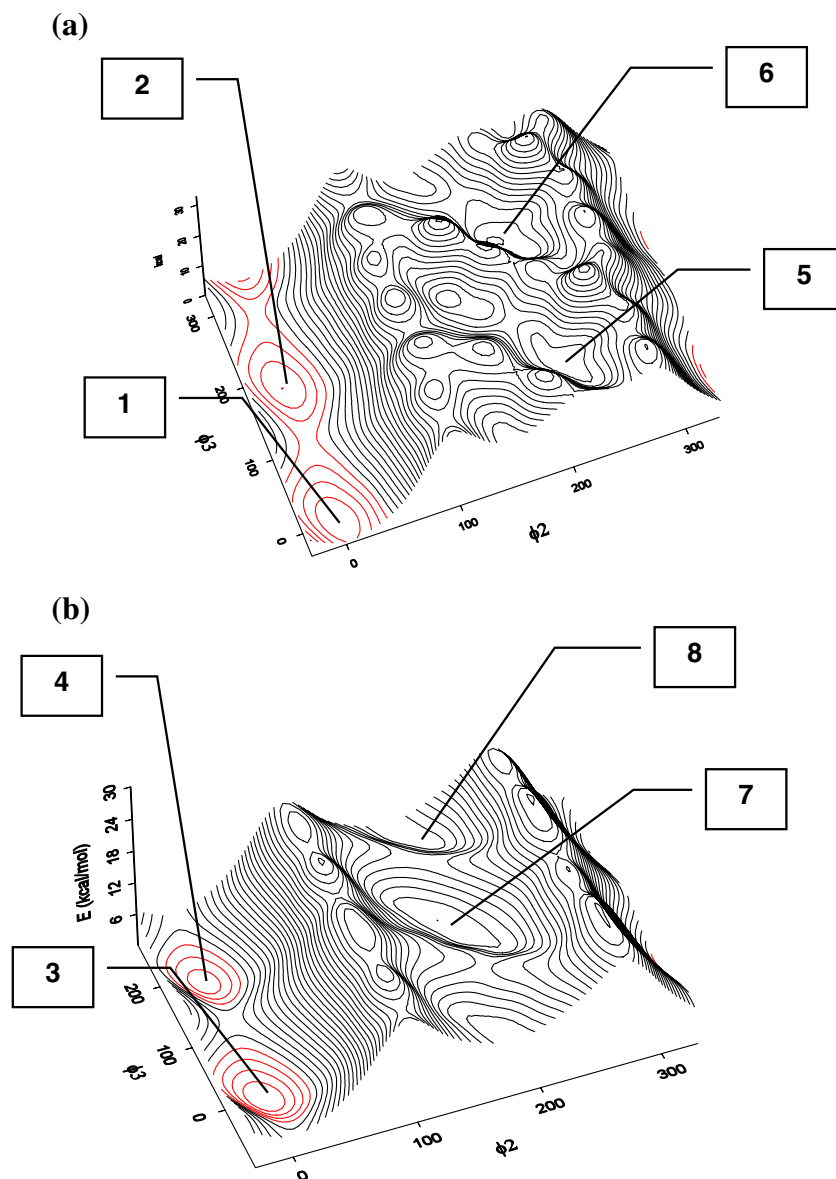


**Figure 2.** Contour graphic of the PES obtained for compound **2a** from RHF/3-21G calculations. In figure 2a the torsional angle  $\phi_1$  adopts values near to zero and in Figure 2b near to 180°. Full cycle of rotation (from 0° to 360°) is shown for variables  $\phi_2$  and  $\phi_3$ . The iso-energy curves included in an energy window of 4 Kcal/mol are denoted in red.

the various conformers are correct, we performed more accurate DFT (B3LYP/6-31G(d)) calculations. With them, we evaluated the molecular flexibility of compound **2a** generating 1-D cross-sections, that is potential energy curves, along  $\phi_2$  and  $\phi_3$  (Fig. 3). To understand the significance of the rotation barriers, it is important to look not just at the magnitudes of the energy barriers, but at the complete energy versus rotation angle behavior. By looking first the torsional angle  $\phi_2$ , we see that the energy minima occur at  $\phi_2 = 18, 150, 210$  and  $345^\circ$ , the quasi-planar conformations, while the energy maxima occur near to  $90$  and  $270^\circ$ , the perpendicular forms. This profile can be understood by recognizing that the planar conformation is stabilized by resonance structures which permit the conjugated  $\pi$ -electron system to delocalize the molecular system. When the torsional angle  $\phi_2$  is rotated almost  $90^\circ$ , resonance stabilization is eliminated, and there is an increase in energy. This increase due to the loss of resonance energy is responsible, at least in part, for the approximately 7 Kcal/mol rotation barriers seen in Figure 3. This barrier indicates that this rotation is somewhat restricted. In contrast, the rotation barrier

**Table 4**

Different conformations of compound **2a** obtained from B3LYP/6-31G(d) optimizations

Conf	Torsional Angles			Energy Gap $\Delta E$ (Kcal.mol <sup>-1</sup> )
	$\phi_1$	$\phi_2$	$\phi_3$	
1	180.0	0.0	0.0	0.00
2	179.97	0.0	180.1	0.65
3	0.0	0.0	0.0	4.53
4	0.0	0.0	180.0	5.12
5	172.33	146.31	169.71	13.54
6	172.63	145.84	344.5	13.73
7	352.8	156.52	152.8	14.19
8	7.17	203.49	207.17	14.19

displayed for torsional angle  $\phi_3$  is very low (less than 1 Kcal/mol, Fig. 3). Although the minima for  $\phi_3$  are located near to  $90$  and  $270^\circ$ , DFT calculations predicts that this is practically a free rotation and therefore different conformations might be adopted for  $\phi_3$  without a significant energy requirement. In Table 4, the differ-

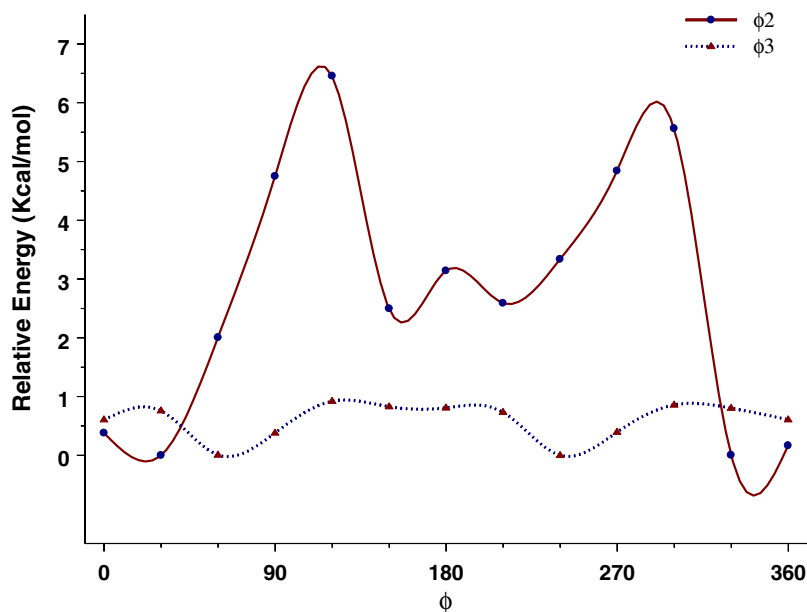


**Figure 3.** Potential Energy Curves (PECs) obtained for the torsional angles  $\phi_2$  and  $\phi_3$  of compound **2a**. Each PEC was calculated at B3LYP/6-31G (d) level of theory.

ent conformers obtained for compound **2a** optimized from B3LYP/6-31G(d) calculations, are summarized.

The conformational behavior of compound **2b** is mainly determined by six torsional angles ( $\Phi_1$ – $\Phi_6$ , Fig. 1b). As we expected, the conformational behaviors obtained for  $\Phi_1$  and  $\Phi_2$  are very similar to those observed for the torsional angles  $\Phi_1$  and  $\Phi_2$  of compound **2a**. The nitroso group adopts only two forms (near to  $0^\circ$  and near to  $180^\circ$ ), whereas the potential energy curve obtained for the dihedral angle  $\Phi_2$  is closely related to that attained for  $\Phi_2$  of compound **2a**. The rest of the torsional angles displayed rotation barriers lower than 3 kcal/mol suggesting that the hydrocarbon side-chain of compound **2b** is flexible enough to adopt different conformations, from a folded form to an extended one. To categorize the obtained structures, we introduced, intuitively rather than by a precise definition, four forms: fully folded (FF), open folded (OF), and fully extended (FE). By FF form we understand a close structure with the flexible side chain (butyl group) completely folded. By FE form we understand a form with a linearized connecting chain. By OF we denote a form intermediate between folded and extended. Figure 1b shows a spatial view of the lowest-energy conformation obtained for compound **2b**; note that, in this conformer, the flexible side chain displayed a partially folded spatial ordering.

Compound **5** possesses a very restricted molecular flexibility being a spatial ordering with  $\Phi_2$  near to  $60^\circ$  the highly preferred conformer. In fact, this molecule possesses three equivalent conformations with  $\Phi_2$  near to  $60^\circ$ ,  $180^\circ$  and  $300^\circ$ . It is clear, however, that the conformational interconversion is a restricted process. DFT calculations predict an energy barrier of more than 7.8 Kcal/mol for such process. As it was previously discussed, this restricted molecular flexibility might be, at least in part, responsible for the lower antifungal activity obtained for this compound in comparison to **2a** and **2b**.

It should be noted that compound **14** was the only active compound possessing a central aromatic ring different to that of compounds type **2** or **5**. Unfortunately this compound displayed a high acute toxicity in comparison with compounds **2a** and **2b**. Thus, we hypothesize that one of the potentially responsible groups for such effect could be the oxygen atom at the connecting chain in **14**. With the aim to design a new compound possessing a central ring similar to **14** but on the other hand with similar structural feature to that of

compound **2a**, we evaluated the conformational properties of a hypothetical compound **15**. Note that in this compound the  $-O-CH_2-$  connecting chain was replaced by  $-NH-$  trying to mimic compound **2a**. As we expected, the conformational behavior obtained for compound (named compound **15**) was very similar to that attained for **2a**. The potential energy curves obtained for the torsional angles  $\Phi_2$  and  $\Phi_3$  of compound **15** are shown in Figure 4.

Next, we performed a comparative conformational study of compounds **2a**, **2b** and **5**. In this comparative analysis, we also included the hypothetical compounds **15**. Figure 5 shows a spatial view of the superimposed conformations of these compounds. From this figure, it is clear that compound **15** can adopt spatial dispositions very similar to those of the active compounds **2a**, **2b** and **5**.

It is clear that not only the conformational aspects but the electronic properties of these compounds are determinant for the antifungal activities. Thus, the knowledge of the stereo-electronic attributes and properties of these nitrosopyrimidines will contribute significantly to the elucidation of the structural requirements to produce the antifungal activity. Molecular electrostatic potentials (MEP) are of particular value because they allow the visualization and assessment of the capacity of a molecule to interact electrostatically with a putative-binding site.<sup>38–40</sup> MEP can be interpreted in terms of a stereo-electronic pharmacophore condensing all available information on the electrostatic forces underlying affinity and specificity. More positive potentials reflect nucleus predominance, while less positive values represent rearrangements of electronic charges and lone pairs of electrons. The fundamental application of this study is the analysis of non-covalent interactions,<sup>40</sup> mainly by investigating the electronic distribution in the molecule. Thus, this methodology was used to evaluate the electronic distribution around molecular surface for compounds reported here.

Figure 6 gives the Molecular Electrostatic Potentials (MEPs) obtained for compounds **2a**, **2b**, **5** and **15**. The MEPs obtained for compounds **2a**, **2b** and **15** account for the general characteristics of the electronic behaviour for the active compounds. The general pattern is very similar for all these systems. The MEPs exhibit four characteristic regions: a clear minimum value (deep red zone with  $V(r)_{\min} \approx -0.0874$  e/au<sup>3</sup>) in the vicinity of the NO group; two positive regions (deep blue zones with  $V(r)_{\max} \approx 0.054$  e/au<sup>3</sup>) located near to the NH<sub>2</sub> and OCH<sub>3</sub> groups and an extended hydrophobic

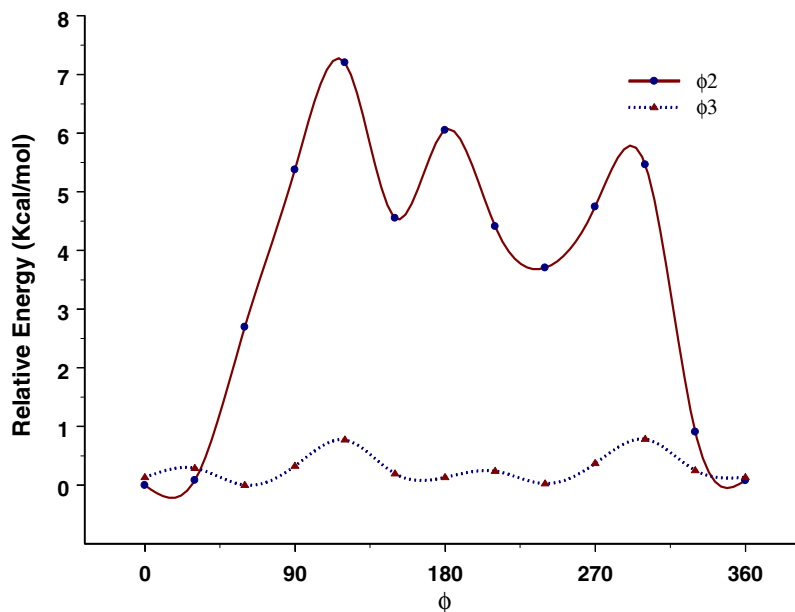


**Figure 4.** Potential Energy Curves (PECs) obtained for the torsional angles  $\phi_2$  and  $\phi_3$  of compound **15**. Each PEC was calculated at B3LYP/6-31G (d) level of theory.

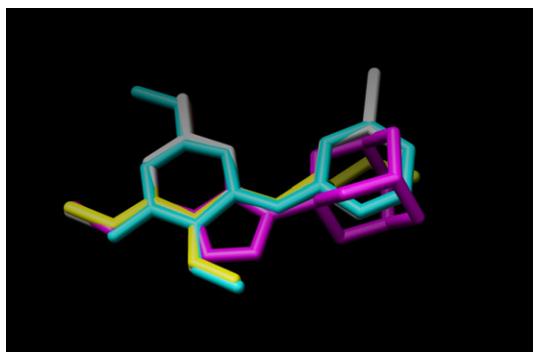


**Figure 5.** Stereoview of overlapping of global minima for **2a** (light blue), **2b** (yellow), **5** (fuchsia) and **15** (green).

zone (deep and light green zone with an almost a neutral potential  $V(r)_{\text{med}} \approx -0.0022 \text{ e/a.u.}^3$ ) throughout the second ring (or the flexible side chain in the case of compound **2b**). It should be noted that the MEP obtained for compound **14** displayed the general characteristics observed for all the active molecules in this series. This MEP is shown in figure 1S as Supplementary material.

The MEP obtained for compound **5** displayed some differences with respect to those of the compounds **2a**, **2b**. This MEP does not show a deep red zone; displaying a generalized hydrophobic potential. The different electronic behavior added to the restricted molecular flexibility could explain the lower antifungal activity obtained for this compound with respect to the active molecules **2a** and **2b**.

From Figure 6 it is clear that compounds **2a**, **2b** and **15** displayed a closely related electronic distribution. Thus, our theoretical calculations indicated that compound **15** possesses a similar stereo-electronic behavior in comparison with the active compounds **2a** and **2b**.

#### 2.4. Experimental support for the theoretical calculations

Our molecular modeling study indicated that compound **15** possesses the minimal structural characteristics to produce the antifungal effect. Thus, in the next step of our study we decided

to synthesize (see Chemistry section) and to test the antifungal activity for this compound in order to corroborate the results obtained from our theoretical study. Interestingly enough, compound **15** displayed the strongest antifungal activity obtained for this series. This compound displayed 76 % inhibition at a relatively low molar concentration (3.9  $\mu\text{g/mL}$ ) possessing a  $\text{MIC}_{50} = 1.9 \mu\text{g/mL}$  against *C. Neoformans*. Similar results were obtained against the other two fungi tested here (Table 2). It is clear that these experimental results are in a complete agreement with our theoretical results and give support to the molecular modeling study.

We evaluated the acute toxicity of this new compound. Our results indicated that compound **15** displayed just a moderate acute toxicity; being non toxic (0% mortality) at 35  $\mu\text{g/mL}$ . Although this toxicity is markedly lower than that previously obtained for compound **14** (non-toxic at 5  $\mu\text{g/mL}$ ), the acute toxicity obtained for compound **15** is still significant and could be a limitation for the potential usefulness of this compound as antifungal agent.

Finally, it is important to highlight that the mechanism of action of these compounds has not been determined yet; therefore it is very difficult to perform a clear and definitive SAR study with this series. Thus, it is prudent to remark that the results of our SAR analysis might be considered like preliminary and exploratory but not definitive ones; however in our opinion these results could be useful to orientate new studies. As was pointed out, unfortunately we have not yet definitive results about the possible molecular mechanism for these nitrosopyrimidines. Different bioassays are being carried out in our laboratories in order to obtain sufficient information regarding this matter. In addition new nitrosopyrimidines are now being synthesized in our laboratory considering the pharmacophoric pattern obtained.

### 3. Conclusions

The synthesis, in vitro evaluation and SAR studies of 32 nitrosopyrimidines and derivatives acting as antifungal agents are reported. A molecular-modeling study using quantum mechanical calculations allowed us to design a new compound possessing the potential parent for this series. Thus, we designed, synthesized and tested compound **15** which displayed the strongest antifungal activity among the nitrosopyrimidines reported here. From our

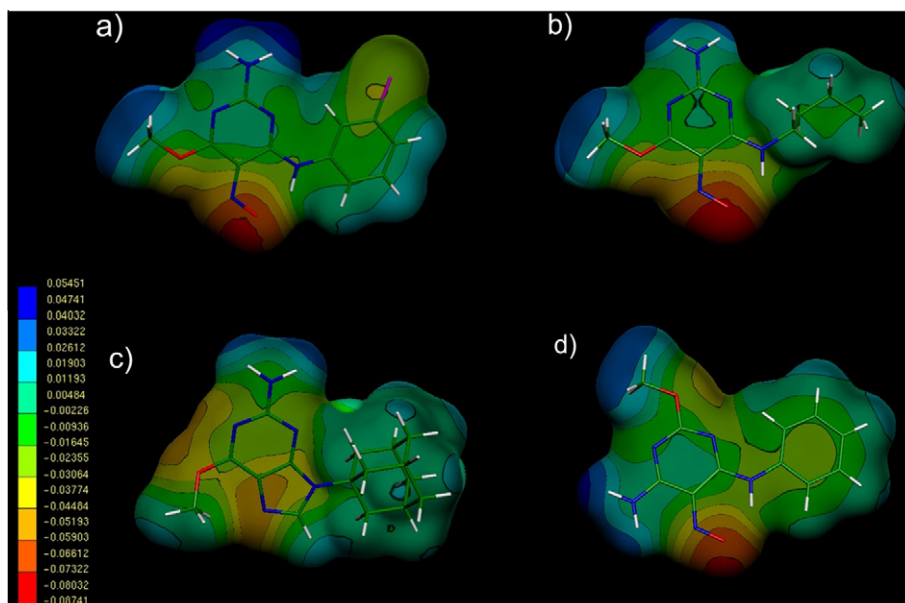


**Figure 6.** Electrostatic potential-encoded electron density surfaces of compounds **2a** (a), **2b** (b), **5** (c) and **15** (d). The surfaces were generated with GAUSSIAN 03 using B3LYP/6-311++G(d,p) single point calculations. The coloring represents electrostatic potential with red indicating the strongest attraction to a positive point charge and blue indicating the strongest repulsion. The electrostatic potential is the energy of interaction of the positive point charge with the nuclei and electrons of a molecule. It provides a representative measure of overall molecular charge distribution. The color-code is shown at the left.

results (antifungal activity and acute toxicity) it appears that compounds **2a**, **2b** and **15** are interesting candidates for further studies.

On the other hand, our SAR study, supported by theoretical calculations, helped us to identify and understand the minimum structural requirements for the antifungal action of these compounds. Thus, we believe that our results could provide a guide in the design of nitrosopyrimidines with this biological activity.

#### 4. Experimental chemistry

Melting points were determined on a *Barstead Electrothermal 9100* apparatus and are uncorrected. IR spectra were recorded in KBr disks on *Bruker TENSOR 27* spectrophotometer from “Centro de Instrumentación Científico-Técnica (CICT) at Universidad de Jaén”.  $^1\text{H}$  and  $^{13}\text{C}$  NMR spectra were recorded on a Bruker Avance 400 spectrophotometer (CICT) operating at 400 MHz and 100 MHz respectively, using  $\text{CDCl}_3$  and  $[\text{D}_6]\text{DMSO}$  as solvents and tetramethylsilane as internal standard; Multiplicity of the carbons was assigned with DEPT and gHSQC experiments, although usual abbreviations according to off-resonance decoupling are used: (s) singlet, (d) doublet, (t) triplet, (q) quartet. The same abbreviations were used for the multiplicity of signals in  $^1\text{H}$  NMR and also: (m) multiplet, (bs) broad singlet. Coupling constants ( $J$ ) are reported in Hertz. Mass spectra were run on a SHIMADZU-GCMS 2010-DI-2010 spectrometer (equipped with a direct inlet probe) operating at 70 eV. High resolution Mass spectra were run on a *Waters Micro-mass AutoSpec-Ultima* spectrometer (equipped with a direct inlet probe) operating at 70 eV. Silica gel aluminum plates (Merck 60 F<sub>254</sub>) were used for analytical TLC. The microwaves assisted reactions were carried out in a 10 mL glass sealed tube for focused mono-mode microwaves oven (“Discover” by CEM Corporation) working at standart mode by controlling the target temperature. The amines, aminoesters, 2-amino-4,6-dimethoxy-pyrimidine, 4-amino-2,6-dimethoxy-pyrimidine were purchased from Aldrich, Fluka and Acros (synthesis reagent grades) and were used without further purification. Solvents were purchased from the same vendors but purified according standard protocols. 6-Amino-2-methoxy-pyrimidin-4(3H)-one and nitrosopyrimidines **1a**, **2a–i**, **3a–g**, **4a–b** were synthesized using reported procedures.<sup>34a</sup>

#### 4.1. Preparation of alkoxy-pyrimidines

##### 2-Amino-4,6-bis-cyclohexylmethoxy-5-nitrosopyrimidine

**1b:** A suspension of 2-amino-4,6-dimethoxy-5-nitroso-pyrimidine **1a** (368 mg, 2.00 mmol) in cyclohexylmethanol (10 mL) was heated at 100 °C until no starting material was visualized by TLC (Silica, eluent:  $\text{CH}_2\text{Cl}_2/\text{MeOH}$  9:1, v/v). Then, solvent was evaporated off by vacuum distillation and hexane was added. The precipitate was filtered, washed and finally, dried in a vacuum dessiccator over potassium hydroxide pellets obtaining compound **1b** as a green solid (557 mg, 80%). mp 165–167 °C.  $^1\text{H}$  NMR (400 MHz,  $\text{DMSO-d}_6$ , 25 °C)  $\delta$  (ppm): 8.18 (bs, 2H,  $\text{NH}_2$ ), 4.20 (d,  $J = 8.3$  Hz, 4H,  $2\text{OCH}_2$ ), 1.80–1.63 (m, 12H,  $\text{CH}_2$ ), 1.31–1.13 (m, 10H, CH,  $\text{CH}_2$ ).  $^{13}\text{C}$  NMR (100 MHz,  $\text{DMSO-d}_6$ )  $\delta$ : 163.0 (s), 141.5 (s), 71.8 (t), 36.6 (d), 29.0 (t), 26.0 (t), 25.2 (t). IR (KBr):  $\nu = 3306$ , 3223, 2937, 1634, 1579, 1357, 1233  $\text{cm}^{-1}$ . UV-vis (MeOH):  $\lambda_{\text{max}}$  nm ( $\log \epsilon$ ) = 239 (4.08), 337 (4.44), 659 (1.80). MS (EI, 70 eV): 348 ( $\text{M}^+$ , 14), 252 (13), 156 (100), 139 (16), 55 (24). HR-MS (EI):  $\text{C}_{18}\text{H}_{28}\text{N}_4\text{O}_3$  requires 348.2161, found 348.2164. Anal. Calcd for  $\text{C}_{18}\text{H}_{28}\text{N}_4\text{O}_3$ : (348.44): C, 62.05; H, 8.10; N, 16.08. Found: C, 61.97; H, 8.14; N, 15.73.

##### 2-(2-Amino-6-cyclohexylmethoxy-5-nitroso-pyrimidin-4-ylamino)-propionic acid ethyl ester **8a**:

To a suspension of **1b** (174 mg, 0.50 mmol) in *t*-BuOH (5 mL), *L*-Alanine ethyl ester hydrochloride (94 mg, 0.60 mmol) and  $\text{Et}_3\text{N}$  (61.3 mg, 0.60 mmol) were added. The mixture was stirred at 60 °C and monitored by TLC (Silica, eluent:  $\text{CH}_2\text{Cl}_2/\text{MeOH}$  9:1, v/v) until no starting material was visualized (18 h). Then, solvent was put off by vacuum distillation and  $\text{CH}_2\text{Cl}_2$  was added on the oil obtained. The organic solution was washed with water ( $3 \times 15$ ) and dried on anhydrous sodium sulfate. Finally, solution was filtered and the solvent was removed under vacuum evaporation to offer an oil which was purified by flash column chromatography on silica gel (eluent:  $\text{CH}_2\text{Cl}_2/\text{Me}_2\text{CO}$  10:0.4, v/v) to render titled compound as a blue oil, (124 mg, 71 %).  $^1\text{H}$  NMR (400 MHz,  $\text{CDCl}_3$ , 25 °C)  $\delta$  (ppm): 11.52 (d,  $J = 7.1$  Hz, 1H, NH), 5.63 (bs, 2H,  $\text{NH}_2$ ), 4.70 (q,  $J = 7.1$  Hz, 1H, NCH), 4.31 (d,  $J = 6.6$  Hz, 2H,  $\text{OCH}_2$ ), 4.14 (q,  $J = 7.1$  Hz, 2H,  $\text{OCH}_2$ ), 1.89–1.64 (m, 7H, CH,  $3\text{CH}_2$ ), 1.44 (d,  $J = 7.7$  Hz, 3H,  $\text{CH}_3$ ), 1.24 (t,  $J = 7.1$  Hz, 3H,  $\text{CH}_3$ ), 1.14–0.92 (m, 2H,  $2\text{CH}_2$ ).  $^{13}\text{C}$  NMR (100 MHz,

CDCl<sub>3</sub>)  $\delta$ : 172.1 (s), 171.8 (s, CO), 163.5 (s), 149.7 (s), 139.2 (s), 73.0 (t), 61.4 (t), 48.9 (d), 37.1 (d), 29.7 (t), 26.3 (t), 25.6 (t), 17.9 (q), 14.1 (q). MS (EI, 70 eV): 351 (M<sup>+</sup>, 88), 182 (74), 166 (68), 140 (100).

**2-(2-Amino-6-cyclohexylmethoxy-5-nitroso-pyrimidin-4-ylamino)-3-phenyl-propionic acid ethyl ester 8b:** To a suspension of **1b** (174 mg, 0.50 mmol) in *t*-BuOH (5 mL), *L*-phenylalanine ethyl ester hydrochloride (139 mg, 0.60 mmol) and Et<sub>3</sub>N (61.3 mg, 0.60 mmol) were added. The mixture was stirred at 60 °C and monitored by TLC (Silica, eluent: CH<sub>2</sub>Cl<sub>2</sub>/MeOH 9:1, v/v) until no starting material was visualized (12 h). Then, solvent was put off by vacuum distillation and dichloromethane was added on the oil obtained. The organic solution was washed with water (3 × 15) and dried over anhydrous sodium sulfate. Finally, solution was filtrated and the solvent was removed under vacuum evaporation to offer an oil which was purified by flash column chromatography on silica gel (eluent: CH<sub>2</sub>Cl<sub>2</sub>/Me<sub>2</sub>CO 10:0.4, v/v) to render titled compound as a blue oil (203 mg, 95 %). <sup>1</sup>H NMR (400 MHz, DMSO-d<sub>6</sub>, 25 °C)  $\delta$  (ppm): 11.55 (d, *J* = 7.1 Hz, 1H, NH), 7.39–7.32 (m, 5H, Ph), 5.54 (bs, 2H, NH<sub>2</sub>), 4.93 (dt, *J* = 7.7, 5.5 Hz, 1H, NCH), 4.31 (d, *J* = 6.6 Hz, 2H, OCH<sub>2</sub>), 4.11 (q, *J* = 7.1 Hz, 2H, OCH<sub>2</sub>), 3.21–3.05 (dd, *J* = 7.7, 7.1 Hz, 2H, CH<sub>2</sub>), 1.90–1.67 (m, 7H, CH, 3CH<sub>2</sub>), 1.19 (t, *J* = 7.1 Hz, 3H, CH<sub>3</sub>), 1.30–0.96 (m, 2H, 2CH<sub>2</sub>). <sup>13</sup>C NMR (100 MHz, DMSO-d<sub>6</sub>)  $\delta$ : 172.1 (s), 170.5 (s, CO), 163.4 (s), 149.7 (s), 139.2 (s), 135.8 (s), 129.2 (t), 128.6 (s), 127.1 (t), 122.9 (d), 73.0 (t), 61.4 (t), 54.7 (d), 38.1 (t), 37.1 (d), 29.7 (t), 26.3 (t), 25.6 (t), 14.1 (q). MS (EI, 70 eV): 427 (M<sup>+</sup>, 1), 352 (100), 256 (21), 182 (79), 166 (69), 149 (33), 140 (88), 55 (71).

**2-(4-Methoxy-5-nitroso-6-phenylamino-pyrimidin-2-ylamino)-ethanol 11a:** To a solution of commercial 2-chloro-4,6-dimethoxy-pyrimidine **I** (712 mg, 4.00 mmol) in *t*-BuOH (10 mL), 2-aminoethanol (0.5 mL, 4.0 mmol) was added. The mixture was stirred at 85 °C and monitored by TLC (Silica, eluent: CH<sub>2</sub>Cl<sub>2</sub>/MeOH 9:1, v/v) until no starting material was visualized (18 h). Then, the solvent was eliminated by vacuum distillation and diethylether was added to the oil obtained. The organic solution was washed with water (3 × 15), dried on anhydrous sodium sulfate and finally concentrated to an oily residue which was purified by flash column chromatography on silica gel (eluent: CH<sub>2</sub>Cl<sub>2</sub>/MeOH 10:0.4, v/v) to render 2-(4,6-dimethoxy-pyrimidin-2-ylamino)-ethanol **II** as a yellow oil (606 mg, 76%). <sup>1</sup>H NMR (400 MHz, CDCl<sub>3</sub>, 25 °C)  $\delta$  (ppm): 5.50 (bs, 2H, OH, NH), 5.39 (s, 1H, CH), 3.81 (s, 6H, 2OCH<sub>3</sub>), 3.82–3.76 (q, *J* = 4.9 Hz, CH<sub>2</sub>), 3.57–3.52 (q, *J* = 5.5 Hz, CH<sub>2</sub>). <sup>13</sup>C NMR (100 MHz, CDCl<sub>3</sub>)  $\delta$ : 172.1 (s), 162.2 (s), 79.0 (d), 63.2 (t), 53.7 (q), 44.3 (t). MS (EI, 70 eV): 199 (M<sup>+</sup>, 20), 168 (100), 155 (23), 139 (18), 69 (63).

Compound **II** (199 mg, 1.0 mmol) was dissolved in DMSO (2.5 mL) and isoamyl nitrite was added (14 mg, 1.2 mmol). The mixture was stirred at room temperature and monitored by TLC (Silica, eluent: CH<sub>2</sub>Cl<sub>2</sub>/MeOH 9:1, v/v) until no starting material was visualized (12 h). Then, H<sub>2</sub>O (25 mL) was added with continuous stirring and 30 min later, aniline (3 mmol) was also added. After 18 h, the precipitate was filtered, washed and finally, dried in a vacuum dessiccator over potassium hydroxide pellets offering titled compound as an orange oil (72 mg, 25 %). <sup>1</sup>H NMR (400 MHz, DMSO-d<sub>6</sub>, 25 °C)  $\delta$  (ppm): 13.70, 13.35 (bs, 1H, NH), 9.02 (bs, 1H, NH), 7.70 (m, 2H, Ph), 7.39 (m, 2H, Ph), 7.16 (m, 1H, Ph), 4.74 (bs, 1H, OH), 4.11, 4.09 (s, 3H, OCH<sub>3</sub>), 3.56 (m, 2H, OCH<sub>2</sub>), 3.41 (m, 2H, NCH<sub>2</sub>). <sup>13</sup>C NMR (100 MHz, DMSO-d<sub>6</sub>)  $\delta$ : 170.4, 170.3 (s), 162.0, 161.6 (s), 147.4, 147.1 (s), 138.4, 138.3 (s), 137.3, 137.0 (s), 129.1 (d), 125.2, 125.0 (d), 122.8 (d), 62.2, 62.0 (t), 54.5 (q), 41.1, 41.0 (t). IR (KBr):  $\nu$  = 3366, 3263, 1586, 1562, 1484 cm<sup>-1</sup>. MS (EI, 70 eV): 289 (M<sup>+</sup>, 50), 272 (18), 254 (13), 227 (20), 77 (100), 69 (34), 43 (57). HR-MS (EI): C<sub>13</sub>H<sub>15</sub>N<sub>5</sub>O<sub>3</sub> requires 289.2899, found 289.2889.

Acetic acid 2-(4-methoxy-5-nitroso-6-phenylamino-pyrimidin-2-ylamino)-ethyl ester **11b** and Acetic acid 2-[4-(3-chloro-phe-

nylamino)-6-methoxy-5-nitroso-pyrimidin-2-ylamino]-ethyl ester **11c:** To a suspension of **II** (712 mg, 4.00 mmol) in anhydride acetic (2.5 mL), a drop of acetic acid was added. The mixture was stirred at room temperature and monitored by TLC (Silica, eluent: CH<sub>2</sub>Cl<sub>2</sub>/MeOH 9:1, v/v) until no starting material was visualized (18 h). Then, cold water was slowly added and next, aqueous solution was neutralised with solid sodium hydrogen carbonate and extracted with diethyl ether (3 × 15). Organic phases were combined, dried on anhydrous sodium sulfate and finally concentrated to give an oily residue (683 mg, 2.83 mmol, 71%). This oil was nitrated following the general procedure<sup>34a</sup> to afford a green solid (497 mg, 65%). mp 178–180 °C (d). <sup>1</sup>H NMR (400 MHz, DMSO-d<sub>6</sub>, 25 °C)  $\delta$  (ppm): 8.93 (t, *J* = 5.5 Hz, 1H, NH), 4.17 (t, *J* = 5.5 Hz, 2H, OCH<sub>2</sub>), 3.98 (s, 3H, OCH<sub>3</sub>), 3.96 (s, 3H, OCH<sub>3</sub>), 3.62 (q, *J* = 5.5 Hz, 2H, NCH<sub>2</sub>), 1.99 (s, 3H, CH<sub>3</sub>). <sup>13</sup>C NMR (100 MHz, DMSO-d<sub>6</sub>)  $\delta$ : 170.3 (s, CO), 161.0 (s), 141.5 (s), 62.0 (t), 54.3 (q), 40.4 (t), 20.7 (q). MS (EI, 70 eV): 270 (M<sup>+</sup>, 12), 166 (5), 122 (7), 87 (42), 43 (100).

To obtain compound **11b**, Aniline (93 mg, 1.0 mmol) was added to a suspension of the above green solid (90 mg, 0.33 mmol) in H<sub>2</sub>O/MeOH (6 mL, 2:1, v/v). The mixture was stirred at room temperature and monitored by TLC (Silica, eluent: CH<sub>2</sub>Cl<sub>2</sub>/MeOH 9:1, v/v) until no starting material was visualized (24 h). Then, the precipitate was filtered, washed and finally, dried in a vacuum dessiccator over potassium hydroxide pellets offering titled compound as an orange solid (58 mg, 53%). mp 128–130 (d). <sup>1</sup>H NMR (400 MHz, DMSO-d<sub>6</sub>, 25 °C)  $\delta$  (ppm): 13.68, 13.30 (bs, 1H, NH), 8.99 (bs, 1H, NH), 7.73 (m, 2H, Ph), 7.38 (m, 2H, Ph), 7.18 (m, 1H, Ph), 4.18 (m, 2H, OCH<sub>2</sub>), 4.12, 4.09 (s, 3H, OCH<sub>3</sub>), 3.71 (s, 1H, NCH<sub>2</sub>), 3.60 (s, 1H, NCH<sub>2</sub>), 2.00, 1.90 (s, 3H, CH<sub>3</sub>). <sup>13</sup>C NMR (100 MHz, DMSO-d<sub>6</sub>)  $\delta$ : 171.0 (s, CO), 170.4, 170.3 (s), 162.0, 161.7 (s), 147.4, 147.0 (s), 138.4, 138.3 (s), 137.2, 136.9 (s), 129.0 (d), 125.1, 124.9 (d), 122.8 (d), 62.3, 62.0 (t), 54.5 (q), 41.1, 41.0 (t), 20.8, 20.7 (q). IR (KBr):  $\nu$  = 3193, 2964, 1740, 1586, 1559, 1165 cm<sup>-1</sup>. MS (EI, 70 eV): 331 (M<sup>+</sup>, 13), 272 (3), 254 (2), 227 (5), 87 (9), 43 (100). HR-MS (EI): C<sub>15</sub>H<sub>17</sub>N<sub>5</sub>O<sub>4</sub> requires 331.1281, found 331.1284.

To obtain compound **11c**, 3-Chloroaniline (127 mg, 1.0 mmol) was added to a suspension of the above green solid (90 mg, 0.33 mmol) obtained in H<sub>2</sub>O/MeOH (6 mL, 2:1, v/v). The mixture was stirred at room temperature and monitored by TLC (Silica, eluent: CH<sub>2</sub>Cl<sub>2</sub>/MeOH 9:1, v/v) until no starting material was visualized (36 h). Then, the precipitate was filtered, washed and finally, dried in a vacuum dessiccator over potassium hydroxide pellets offering titled compound as an orange solid (70 mg, 58%), mp 153–155 °C (d). <sup>1</sup>H NMR (400 MHz, DMSO-d<sub>6</sub>, 25 °C)  $\delta$  (ppm): 13.56, 13.27 (bs, 1H, NH), 9.09 (bs, 1H, NH), 8.09 (m, 1H, C<sup>2</sup>Ph), 7.57 (dd, *J* = 7.8, 7.4 Hz, 1H, C<sup>4</sup>Ph), 7.36 (q, *J* = 8.3 Hz, 1H, C<sup>5</sup>Ph), 7.21 (m, 1H, C<sup>6</sup>Ph), 4.23, 4.20 (t, *J* = 5.6 Hz, 2H, OCH<sub>2</sub>), 4.15, 4.11 (s, 3H, OCH<sub>3</sub>), 3.72, 3.62 (q, *J* = 5.7 Hz, 2H, NCH<sub>2</sub>), 2.02, 1.97 (s, 3H, CH<sub>3</sub>). <sup>13</sup>C NMR (100 MHz, DMSO-d<sub>6</sub>)  $\delta$ : 170.3, 170.2 (s), 162.0, 161.7 (s), 147.3 (s), 146.9 (s), 138.7 (s), 138.4 (s), 133.2 (s), 133.1 (s), 130.4, 130.7 (d), 124.7, 124.6 (d), 122.8, 122.5 (d), 121.3 (d), 62.3, 61.9 (t), 54.5 (q), 40.6, 40.4 (t), 20.7, 20.6 (q). IR (KBr):  $\nu$  = 3255, 11741, 1580, 1241 cm<sup>-1</sup>. MS (EI, 70 eV): 365 (M<sup>+</sup>, 66), 306 (12), 288 (9), 261 (16), 111 (14), 87 (47), 43 (100). HR-MS (EI): C<sub>15</sub>H<sub>16</sub>ClN<sub>5</sub>O<sub>4</sub> requires 365.0891, found 365.0898.

**4-Amino-2-methoxy-5-nitroso-6-pyrrolidin-1-yl-pyrimidine 12:** To a suspension of 4-amino-2,6-dimethoxy-5-nitroso-pyrimidine **1c** (184 mg, 1.00 mmol) in dichloromethane (10 mL), pyrrolidine (0.10 mL, 1.1 mmol) was added. The mixture was stirred at room temperature and monitored by TLC (Silica, eluent: CH<sub>2</sub>Cl<sub>2</sub>/MeOH 9:1, v/v) until no starting material was visualized (15 h). Then, water (20 mL) was added and the organic phase was separated and dried on anhydrous sodium sulfate. The solid was removed and the solvent was eliminated, offering titled compound as a blue solid (145 mg, 65%), mp 202–204 °C (d). <sup>1</sup>H NMR (400 MHz, DMSO-d<sub>6</sub>, 25 °C)  $\delta$  (ppm): 10.72 (bs, 1H, NH<sub>2</sub>), 8.34

(bs, 1H, NH<sub>2</sub>), 3.85 (s, 7H, 2NCH<sub>2</sub>, OCH<sub>3</sub>), 1.98–1.91 (M, 4H, 2CH<sub>2</sub>). <sup>13</sup>C NMR (100 MHz, DMSO-d<sub>6</sub>) δ: 164.9 (s), 161.4 (s), 151.2 (s), 142.5 (s), 54.3 (q), 53.0 (t), 50.3 (t), 26.2 (t), 23.0 (t). IR (KBr): ν = 3237, 3051, 1613, 1554, 1251 cm<sup>-1</sup>. MS (EI, 70 eV): 223 (M<sup>+</sup>, 9), 206 (100), 166 (36), 149 (20). HR-MS (EI): C<sub>9</sub>H<sub>13</sub>N<sub>5</sub>O<sub>2</sub> requires 223.1069, found 223.1079.

**6-Amino-3-benzyl-2-methoxy-5-nitroso-pyrimidin-4(3H)-one 13 and 4-Amino-6-benzyl-2-methoxy-5-nitroso-pyrimidine 14:** A suspension of 6-amino-2-methoxypyrimidin-4(3H)-one **III** (10.0 g, 70.85 mmol) and K<sub>2</sub>CO<sub>3</sub> (11.75 g, 85.02 mmol) in DMSO (90 mL) was stirred at room temperature for 30 min. Benzyl chloride (9.9 mL, 85.02 mmol) was then added and the mixture was stirred at room temperature for 18 h. Cold water (270 mL) was added dropwise with continuous stirring and the solid in suspension was then collected by filtration, washed with water and dried in vacuo. The dried solid was suspended in Et<sub>2</sub>O (300 mL) and stirred for 24 h. The solid in suspension was collected by filtration, washed with diethyl ether and recrystallised from methanol to afford the titled compound (5.47 g, 33%) as a white solid which was characterized as 6-amino-3-benzyl-2-methoxypyrimidin-4(3H)-one **IV**, on the other hand, from the ethereal filtrate the *O*-benzyl isomer 6-amino-4-benzyl-2-methoxypyrimidine **V** was recovered (5.67 g, 35%). Finally, compounds **IV** and **V**<sup>34a</sup> (2.31 g, 10.0 mmol) were separately subjected to the general nitrosation procedure<sup>34a</sup> to give compounds **13** and **14**<sup>34a</sup> as blue and green solids respectively (2.47 g, 95 %).

**6-amino-3-benzyl-2-methoxypyrimidin-4(3H)-one IV:** mp 200–202 °C. <sup>1</sup>H NMR (300 MHz, DMSO-d<sub>6</sub>, 25 °C): δ = 7.31–7.18 (m, 5H, Ph), 6.46 (bs, 2H, NH<sub>2</sub>), 4.95 (s, 2H, NCH<sub>2</sub>), 4.89 (s, 1H, CH), 3.82 (s, 3H, OCH<sub>3</sub>) ppm. <sup>13</sup>C NMR (100 MHz, DMSO-d<sub>6</sub>): δ = 162.1 (s), 156.4 (s), 137.6 (s), 128.3 (d), 127.1 (d), 78.9 (d), 55.24 (q), 42.37 (q) ppm. IR (KBr): 3403, 3337, 3197, 1643, 1545, 1395, 1299, 1095 cm<sup>-1</sup>. GC-MS (EI, 70 eV): *m/z* (%) = 231 (M<sup>+</sup>, 100), 214 (16), 125 (36), 111 (8), 104 (30), 91 (93). HR-MS (EI): C<sub>12</sub>H<sub>13</sub>N<sub>3</sub>O<sub>2</sub> requires 231.1002, found 231.1008

**6-Amino-3-benzyl-2-methoxy-5-nitroso-pyrimidin-4(3H)-one 13:** mp 148–150 °C (d). <sup>1</sup>H NMR (400 MHz, DMSO-d<sub>6</sub>, 25 °C): δ = 11.15 (bs, 1H, NH<sub>2</sub>), 9.12 (bs, 1H, NH<sub>2</sub>), 7.33–7.28 (m, 5H, Ph), 5.13 (s, 2H, NCH<sub>2</sub>), 3.99 (s, 3H, OCH<sub>3</sub>) ppm. <sup>13</sup>C NMR (100 MHz, DMSO-d<sub>6</sub>): δ = 161.8 (s), 158.1 (s), 148.3 (s), 142.9 (s), 136.5 (s), 128.5 (d), 127.4 (d), 127.3 (d), 56.8 (q), 43.7 (t) ppm. IR (KBr): ν = 3255, 3034, 1693, 1575, 1504, 1272, 1250, 1058 cm<sup>-1</sup>. GC-MS (EI, 70 eV): *m/z* (%) = 260 (M<sup>+</sup>, 20), 132 (13), 91 (100). UV-vis (MeOH): λ<sub>max</sub> nm (log ε) = 205 (4.28), 229 (4.27), 305 (sh), 335 (4.10), 617 (1.77). HR-MS (EI): C<sub>12</sub>H<sub>12</sub>N<sub>4</sub>O<sub>3</sub> requires 260.0909, found 260.0918.

**4-Amino-6-phenylamino-2-methoxy-5-nitrosopyrimidine 15:** To a suspension of 4-amino-2,6-dimethoxy-5-nitroso-pyrimidine **1c** (184 mg, 1.00 mmol) in water (10 mL), aniline (0.18 mL, 2.0 mmol) was added. The mixture was stirred at room temperature and monitored by TLC (Silica, eluent: CH<sub>2</sub>Cl<sub>2</sub>/MeOH 9:1, v/v) until no starting material was visualized (24 h). Then, the precipitate was filtered, washed and finally, dried in a vacuum desiccator over potassium hydroxide pellets offering titled compound as a green solid (147 mg, 60%), mp 195–197 °C. <sup>1</sup>H NMR (400 MHz, DMSO-d<sub>6</sub>, 25 °C) δ (ppm): 13.56, 9.15 (s, 1H, NH), 10.99, 8.69 (bs, 1H, NH<sub>2</sub>), 10.37, 8.34 (bs, 1H, NH<sub>2</sub>), 7.90–7.75 (dd, *J* = 8.2, 6.7 Hz, 2H, Ph), 7.42–7.35 (m, 2H, Ph), 7.21–7.12 (m, 1H, Ph), 3.91, 3.88 (s, 3H, OCH<sub>3</sub>). <sup>13</sup>C NMR (100 MHz, DMSO-d<sub>6</sub>) δ: 167.6, 167.2 (s), 163.3 (s), 149.7, 146.9 (s), 138.6, 138.1 (s), 137.6, 136.6 (s), 129.0, 128.4 (d), 125.3, 124.3 (d), 123.2, 123.1 (d), 55.1, 54.9 (q). IR (KBr): ν = 3363, 3226, 1652, 1566, 1277 cm<sup>-1</sup>. MS (EI, 70 eV): 245 (M<sup>+</sup>, 35), 228 (100), 211 (41), 157 (17), 77 (31). HR-MS (EI): C<sub>11</sub>H<sub>11</sub>N<sub>5</sub>O<sub>2</sub> requires 245.0913, found 245.0914.

## 4.2. Preparation of fused alkoxyprymidines following a reduction/cyclization process

**2-Amino-4-cyclohexylmethoxy-7-methyl-7,8-dihydro-5H-pteridin-6-one 9a:** To a suspension of nitrosopyrimidine **8a** (96 mg, 0.27 mmol) in MeCN/H<sub>2</sub>O (15 mL, 2:1, v/v) at 50 °C, Na<sub>2</sub>S<sub>2</sub>O<sub>4</sub> (235 mg, 1.35 mmol) was slowly added until decoloration. Then, the mixture was evaporated to dryness, the residue was suspended in water and left at 4 °C overnight. The precipitate was filtered, washed with water and dried over blue silica offering finally titled compound as a pale solid (51 mg, 65%), mp 193–195 °C. <sup>1</sup>H NMR (400 MHz, CDCl<sub>3</sub>, 25 °C) δ (ppm): 7.32 (bs, 1H, NH), 4.87 (bs, 1H, NH), 4.55 (bs, 2H, NH<sub>2</sub>), 4.16 (q, *J* = 7.1, 6.6 Hz, 1H, CHCO), 4.05 (d, *J* = 6.6 Hz, 2H, OCH<sub>2</sub>), 1.78–1.67 (m, 5H, CH, 2CH<sub>2</sub>), 1.46 (d, *J* = 7.1 Hz, 3H, CH<sub>3</sub>), 1.30–1.14 (m, 3H, CH, 3CH<sub>2</sub>), 1.03–0.87 (m, 3H, CH, 3CH<sub>2</sub>). <sup>13</sup>C NMR (100 MHz, CDCl<sub>3</sub>) δ: 165.2 (s, CO), 157.0 (s), 156.2 (s), 151.4 (s), 94.8 (s), 71.6 (t), 51.9 (d), 37.4 (d), 29.7 (t), 26.4 (t), 25.7 (t), 19.6 (q). IR (KBr): ν = 3376, 3220, 2926, 1651, 1599, 1472 cm<sup>-1</sup>. MS (EI, 70 eV): 291 (M<sup>+</sup>, 32), 195 (100), 180 (48), 152 (41). HR-MS (EI): C<sub>14</sub>H<sub>21</sub>N<sub>5</sub>O<sub>2</sub> requires 291.1695, found 291.1708.

**2-Amino-7-benzyl-4-cyclohexylmethoxy-7,8-dihydro-5H-pteridin-6-one 9b:** To a suspension of nitrosopyrimidine **8b** (72 mg, 0.17 mmol) in MeCN/H<sub>2</sub>O (15 mL, 2:1, v/v) at 50 °C, Na<sub>2</sub>S<sub>2</sub>O<sub>4</sub> (148 mg, 0.85 mmol) was slowly added until decoloration. Then, the mixture was evaporated to dryness, the residue was suspended in water and left at 4 °C overnight. The precipitate was filtered, washed with water and dried over blue silica offering finally titled compound as a pale solid (47 mg, 75%) mp 213–215 °C. <sup>1</sup>H NMR (400 MHz, CDCl<sub>3</sub>, 25 °C) δ (ppm): 7.34–7.20 (M, 6H, NH, Ph), 4.89 (bs, 1H, NH), 4.57 (bs, 2H, NH<sub>2</sub>), 4.30–4.26 (ddd, *J* = 7.1, 6.6 Hz, 1H, CHCO), 4.04 (d, *J* = 6.6 Hz, 2H, OCH<sub>2</sub>), 3.38–3.32 (dd, *J* = 13.7, 3.3 Hz, 1H, CH<sub>2</sub>), 2.94–2.86 (dd, *J* = 13.7, 9.9 Hz, 1H, CH<sub>2</sub>), 1.78–1.68 (m, 5H, CH, 2CH<sub>2</sub>), 1.34–1.16 (m, 4H, 2CH<sub>2</sub>), 1.05–0.87 (m, 2H, CH<sub>2</sub>). <sup>13</sup>C NMR (100 MHz, CDCl<sub>3</sub>) δ: 164.1 (s, CO), 157.7 (s), 156.2 (s), 150.7 (s), 136.0 (s), 129.5 (d), 129.0 (d), 127.3 (d), 94.6 (s), 71.7 (t), 57.5 (d), 39.5 (t), 37.4 (d), 29.7 (t), 26.4 (t), 25.7 (t). IR (KBr): ν = 3354, 3226, 2924, 1677, 1624, 1600, 1468 cm<sup>-1</sup>. MS (EI, 70 eV): 367 (M<sup>+</sup>, 25), 276 (43), 180 (100), 163 (15), 91 (17). HR-MS (EI): C<sub>20</sub>H<sub>25</sub>N<sub>5</sub>O<sub>2</sub> requires 367.2008, found 367.2006.

**2-Amino-4-methoxy-5,7,8,9-tetrahydro-pyrimido[4,5-b][1,4]diazepin-6-one 10:** To a suspension of 3-(2-amino-6-methoxy-5-nitroso-pyrimidin-4-ylamino)-propionic acid ethyl ester **2h**<sup>34a</sup> (269 mg, 1.00 mmol) in MeCN/H<sub>2</sub>O (20 mL, 3:1, v/v) at 50 °C, Na<sub>2</sub>S<sub>2</sub>O<sub>4</sub> (871 mg, 5.00 mmol) was slowly added until decoloration. Then, the mixture was evaporated to dryness, the residue was suspended in water and left at 4 °C overnight. The precipitate was filtered, washed with water and dried over blue silica offering finally titled compound as a pale solid (72 mg 34%), mp 178–180 °C (d). <sup>1</sup>H NMR (400 MHz, DMSO-d<sub>6</sub>, 25 °C) δ (ppm): 8.01 (s, 1H, NH), 6.74 (t, 1H, NH), 5.85 (bs, 2H, NH<sub>2</sub>), 3.41 (m, 2H, NCH<sub>2</sub>), 2.47 (m, 2H, CH<sub>2</sub>), 3.77 (s, 3H, OCH<sub>3</sub>). <sup>13</sup>C NMR (100 MHz, DMSO-d<sub>6</sub>) δ: 171.8 (s, CO), 161.4 (s), 158.3 (s), 155.2 (s), 91.8 (s), 53.2 (q), 41.6 (t), 36.7 (t). IR (KBr): ν = 3388, 3141, 1755, 1652, 1208 cm<sup>-1</sup>. MS (EI, 70 eV): 209 (M<sup>+</sup>, 100), 194 (49), 166 (65), 149 (16). HR-MS (EI): C<sub>8</sub>H<sub>11</sub>N<sub>5</sub>O<sub>2</sub> requires 209.0913, found 209.0921.

## 4.3. Antifungal evaluation

### 4.3.1. Microorganisms and media

For the antifungal evaluation, standardized strains from the American Type Culture Collection (ATCC), Rockville, MD, USA, and Colección de Cultivos de CEREMIC (CCC, Centro de Referencia en Micología, Facultad de Ciencias Bioquímicas y Farmacéuticas, Suipacha 531-(2000)-Rosario, Argentina) were used in a first in-

stance of screening: *C. albicans* ATCC 10231, *Cryptococcus neoformans* ATCC 32264, *Aspergillus flavus* ATCC 9170, *A. fumigatus* ATCC 26934, *A. niger* ATCC 9029, *Trichophyton rubrum* CCC 110, *T. mentagrophytes* ATCC 9972 and *M. gypseum* CCC 115.

Strains were grown on Sabouraud-chloramphenicol agar slants for 48 h at 30 °C, maintained on slopes of Sabouraud-Dextrose agar (SDA, Oxoid) and sub-cultured every 15 days to prevent pleomorphic transformations. Inocula of cell or spore suspensions were obtained according to reported procedures and adjusted to  $1-5 \times 10^3$  cells/spores with colony forming units (CFU)/mL.<sup>36</sup>

#### 4.3.2. Antifungal susceptibility testing

Minimum Inhibitory Concentration (MIC) of each extract or compound was determined by using broth microdilution techniques according to the guidelines of the National Committee for Clinical Laboratory Standards for yeasts (M27-A3) and for filamentous fungi (M 38-A2).<sup>36</sup> MIC values were determined in RPMI-1640 (Sigma, St Louis, Mo, USA) buffered to pH 7.0 with MOPS. Microtiter trays were incubated at 30 °C for yeasts and species of *Aspergillus* and at 28–30 °C for dermatophytes in a moist, dark chamber. MICs were visually recorded at 48 h for yeasts, and at a time according to the control fungus growth, for the rest of fungi.

For the assay, stock solutions of pure compounds were twofold diluted with RPMI from 250–0.98 µg/mL (final volume = 100 µl) and a final DMSO concentration ≤1%. A volume of 100 µl of inoculum suspension was added to each well with the exception of the sterility control where sterile water was added to the well instead. Amphotericin B, Terbinafine and Ketoconazole were used as positive controls.

Endpoints recorded in Table 2 were defined as the lowest concentration of drug resulting in total inhibition (MIC<sub>100</sub>) of visual growth compared to the growth in the control wells containing no antifungal.

#### 4.3.3. MFC determination

The minimum fungicidal concentration (MFC) of each compound against each isolate was also determined as follows: After determining the MIC, an aliquot of 5 µL sample was withdrawn from each clear well of the microtiter tray and plated onto a 150 mm RPMI-1640 agar plate buffered with MOPS (Remel, Lenexa, Kans.). Inoculated plates were incubated at 30 °C, and MFCs were recorded after 48 h. The MFC was defined as the lowest concentration of each compound that resulted in total inhibition of visible growth.

#### 4.3.4. Inhibition percentage determination

The test was performed in 96-well microplates. Compound test wells (CTWs) were prepared with stock solutions of each compound in DMSO (maximum concentration ≤1%), diluted with RPMI-1640 to final concentrations 250–0.98 µg/mL. Inoculum suspension (100 µl) was added to each well (final volume in the well = 200 µl). A growth control well (GCW) (containing medium, inoculum, the same amount of DMSO used in CTW, but compound-free) and a sterility control well (SCW) (sample, medium and sterile water instead of inoculum) were included for each fungus tested. Microtiter trays were incubated in a moist, dark chamber at 30 °C, 24 or 48 h for *C. albicans* or *C. neoformans*, respectively. Microplates were read in a VERSA Max microplate reader (Molecular Devices, Sunnyvale, CA, USA). Amphotericin B was used as positive control.

Tests were performed in duplicate. Reduction of growth for each compound concentration was calculated as follows: % of inhibition =  $100 - ((OD_{405} \text{ CTW} - OD_{405} \text{ SCW}) / (OD_{405} \text{ GCW} - OD_{405} \text{ SCW}))$ .

#### 4.3.5. MIC<sub>50</sub> determination

MIC<sub>50</sub> was defined as the lowest concentration of a compound that showed 80% or 50% reduction of the growth control

respectively and was determined from the results obtained in the inhibition percentage determination.

#### 4.4. Statistical analysis

Data of percentage of inhibition were statistically analyzed by both, one-way analysis of variance and Student's test. A  $p < 0.05$  was considered significant.

#### 4.5. Acute toxicity test

Toxic effect of compounds was evaluated using a toxicity test on fish. The static technique recommended by the US Fish and wildlife Service Columbia National Fisheries Research Laboratory<sup>41</sup> was modified in order to use lower amounts of tested compounds.<sup>37</sup> Fish of the specie *Poecilia reticulata* were born and grown in our laboratory until they reached a size of 0.7–1 cm (15 days-old). In the toxicity test, 10 specimens were exposed to each of the concentration tested per drug in 2 L wide-mouthed jars containing the test solutions. Aqueous stock solutions of pure compounds diluted in DMSO were prepared and added to test chambers to get the final concentrations. The test began upon initial exposure to the compounds and continued for 96 h. The number of dead organisms in each test chamber was recorded and the dead organisms were removed every 24 h; general observations on the conditions of tested organisms were also recorded at this time; however the percentage of mortality was recorded at 96 h. Each experiment was performed two times with three replicates each. We chose this technique because it is fast, economic, and easy to reproduce. This assay has been previously used by our group testing the toxicity of synthetic and natural compounds.<sup>20–37</sup> The species *P. reticulata* has been previously used in acute toxicity test.<sup>42</sup>

#### 4.6. Molecular Modeling

All calculations were carried out using the Gaussian 03 program.<sup>43</sup>

The search for low-energy conformations on the potential energy surface for compounds **2a**, **2b**, **5** and **15** was carried out by using combined *ab initio* (RHF/3-21G) and DFT (B3LYP/6-31G(d)) calculations. Final DFT geometries were obtained from the geometry optimisation jobs. Minima were characterized through harmonic frequency analysis calculated at DFT level. Correlations effects were included using Density Functional Theory (DFT) using the functional of Lee, Yang, and Parr<sup>44,45</sup> as proposed and parameterized by Becke<sup>46,47</sup> (RB3LYP), and the 6-31G(d) basis set.

Double scans were run at 30° intervals, from 0 to 360°, involving both  $\Phi_2$  and  $\Phi_3$  for compounds **2a** and **15** using RHF 3-21G calculations. The graphical presentations of the PESs were generated using the program AXUM 5.0 plotting the total energy values as a dependent variable generated by the double scans over the independent variables  $\Phi_2$  and  $\Phi_3$ . The optimum coordinates of  $\Phi_2$  and  $\Phi_3$  for all possible minima were then visually estimated from the level contours diagrams. Potential energy curves (PEC) for  $\Phi_2$  and  $\Phi_3$  of compounds **2a** and **15** have been obtained via one-dimensional (1D)-scans using RHF/3-21G calculations. The energy has been calculated at 30° intervals of the dihedral angles. The electronic study of compounds **2a**, **2b**, **5** and **15** was carried out using molecular electrostatic potentials (MEPs). MEPs have been shown to provide reliable information, both on the interaction sites of the molecules with point charges and on the comparative reactivities of these sites.<sup>39–41</sup> These MEPs were calculated using B3LYP/6-311G (d,p) wave functions from the MOLEKEL program.<sup>48</sup>

Spatial views shown in Figures **2a**, **2b**, **5**, **14** and **15** were constructed using the UCSF Chimera program<sup>49</sup> as graphic interface.

## Acknowledgments

RDE acknowledges ANPCyT, PICT 2010–1832. SAZ acknowledges ANPCyT, PICT 2010–0608 and UNR BIO 258. Grants from Universidad Nacional de San Luis (UNSL), partially supported this work. Authors thank “Centro de Instrumentación Científico Técnica” and the staff for data collection. The financial support from the Consejería de Economía, innovación y Ciencia (Junta de Andalucía, Spain), the Universidad de Jaén and Ministerio de Ciencia e Innovación (project reference SAF2008–04685–CO2–02) is thanked. RDE is member of the Consejo Nacional de Investigaciones Científicas y Técnicas (CONICET-Argentina) staff.

## Supplementary data

Supplementary data associated with this article can be found, in the online version, at <http://dx.doi.org/10.1016/j.bmc.2012.08.033>.

## References and notes

- Kontoyiannis, D.; Mantadakakis, E.; Samonis, G. *J. Hosp. Infect.* **2003**, *53*, 243.
- Mathew, B.; Nath, M. *Chem. Med. Chem.* **2009**, *4*, 310.
- Monk, B.; Goffeau, A. *Science* **2008**, *321*, 367.
- Sheehan, D. J.; Hitchcock, C. A.; Sibley, C. M. *Clin. Microbiol. Rev.* **1999**, *12*, 40.
- Kullberg, B. J.; De Pauw, B. E. *Neth. J. Med.* **1999**, *55*, 118.
- Pfaller, M.; Messer, S.; Boyken, L.; Rice, C.; Tendolkar, S.; Hollis, R.; Diekema, D. *J. Clin. Microbiol.* **2007**, *45*, 70.
- Mukherjee, P. K.; Chandra, J.; Kuhn, D. M.; Ghannoum, M. A. *Infect Immun.* **2003**, *71*, 4333.
- Espinel-Ingroff, A. *Micol.* **2009**, *26*, 15.
- Johnson, M.; MacDougall, C.; Ostrosky-Zeichner, L.; Perfect, J.; Rex, J. *Antimicrob. Agents Chemother.* **2004**, *48*, 693.
- Cuenca-Estrella, M. *J. Antimicrob. Chemother.* **2004**, *54*, 854.
- Masman, M. F.; Rodríguez, A. M.; Svetaz, L.; Zacchino, S. A.; Somlai, C.; Csizmadia, I. G.; Penke, B.; Enriz, R. D. *Bioorg. Med. Chem.* **2006**, *14*, 7604.
- Masman, M. F.; Somlai, C.; Garibotto, F. M.; Rodríguez, A. M.; de la Iglesia, A.; Zacchino, S. A.; Enriz, R. D. *Bioorg. Med. Chem.* **2008**, *16*, 4347.
- Masman, M. F.; Rodríguez, A. M.; Raimondi, M.; Zacchino, S. A.; Luiten, P. G.; Somlai, C.; Kortvelyesi, T.; Penke, B.; Enriz, R. D. *Eur. J. Med. Chem.* **2009**, *44*, 212.
- Garibotto, F. M.; Garro, A. D.; Somlai, C.; Masman, M. F.; Lutien, P.; Zacchino, S. A.; Rodríguez, A. M.; Penke, B.; Enriz, R. D. *Bioorg. Med. Chem.* **2010**, *18*, 158.
- Olivella, M. S.; Rodríguez, A. M.; Zacchino, S. A.; Somlai, C.; Penke, B.; Farkas, V.; Perczel, A.; Enriz, R. D. *Bioorg. Med. Chem. Lett.* **2010**, *20*, 4808.
- Garibotto, F. M.; Garro, A. D.; Rodríguez, A. M.; Raimondi, M.; Zacchino, S. A.; Somlai, C.; Penke, B.; Enriz, R. D. *J. Med. Chem.* **2011**, *46*, 370.
- Garro, A. D.; Garibotto, F. M.; Rodríguez, A. M.; Raimondi, M.; Zacchino, S. A.; Perczel, A.; Somlai, C.; Penke, B.; Enriz, R. D. *Letts. Drug Des. & Disc.* **2011**, *6*, 562.
- Zacchino, S.; Rodríguez, G.; Pezzenati, G.; Orellana, G.; Enriz, R. D.; Gonzalez Sierra, M. *J. Nat. Prod.* **1997**, *60*, 659.
- Zacchino, S.; López, S. A.; Pezzenati, G.; Furlán, R.; Santecchia, C.; Muñoz, L.; Giannini, F.; Rodríguez, A. M.; Enriz, R. D. *J. Nat. Prod.* **1999**, *63*, 1353.
- Freile, M. L.; Giannini, F.; Pucci, G.; Sturniolo, A.; Doderio, L. R.; Pucci, O.; Balzaretto, V.; Enriz, R. D. *Fitoter.* **2003**, *74*, 702.
- Kurdelas, R. R.; Lima, B.; Tapia, A.; Feresin, G. E.; Sierra, M. G.; Rodríguez, M. V.; Zacchino, S.; Enriz, R. D.; Freile, M. L. *Moléculas* **2010**, *15*, 4898.
- Kouznetsov, V. V.; Urbina, J.; Palma, A.; López, S.; Ribas, J.; Enriz, R. D.; Zacchino, S. *Bioorg. Med. Chem.* **2000**, *8*, 691.
- Lopez, S. N.; Castelli, M. V.; Zacchino, S.; Dominguez, J.; Lobo, G.; Charris-Charris, J.; Cortes, D.; Ribas, J.; Devia, C.; Rodriguez, A. M.; Enriz, R. D. *Bioorg. Med. Chem.* **1999**, *2001*, 9.
- Vargas, L. Y.; Castelli, M.; Kouznetsov, V.; Urbina, J. M.; Lopez, S. N.; Sortino, M.; Enriz, R. D.; Ribas, J. C.; Zacchino, S. *Bioorg. Med. Chem.* **2003**, *11*, 1511.
- Karolyhazy, L.; Freile, M. L.; Anwar, M.; Beke, G.; Giannini, F.; Sortino, M.; Ribas, J. C.; Zacchino, S.; Matyus, P.; Enriz, R. D. *Arzneim.-Forsch./-Drug Res.* **2003**, *53*, 738.
- Giannini, F.; Aymar, L. M.; Sortino, M. V.; Gomez, R.; Sturniolo, A.; Juarez, A.; Zacchino, S.; De Rossi, R. H.; Enriz, R. D. *Il Farm.* **2004**, *59*, 245.
- Lopez, S. N.; Castelli, M. V.; Rogerio Correa, F.; Cechinel Filho, V.; Yunes, R. A.; Zamora, M. A.; Enriz, R. D.; Ribas, J. C.; Zacchino, S. A. *Arzneim.-Forsch./-Drug Res.* **2005**, *55*, 123.
- Suvire, F. D.; Sortino, M.; Kouznetsov, V. V.; Vargas, L. Y.; Zacchino, S.; Mora Cruz, U.; Enriz, R. D. *Bioorg. Med. Chem.* **1851**, *2006*, 14.
- Kouznetsov, V. V.; Vargas Mendes, L. Y.; Sortino Vasquez, M.; Vasquez, Y.; Gupta, M. P.; Freile, M.; Enriz, R. D.; Zacchino, S. *Bioorg. Med. Chem.* **2008**, *16*, 794.
- Sortino, M.; Garibotto, F.; Cechinel Filho, V.; Enriz, R. D.; Zacchino, S. *Bioorg. Med. Chem.* **2011**, *19*(9), 2823.
- Garibotto, F. M.; Sortino, M. A.; Kouznetsov, V. V.; Enriz, R. D.; Zacchino, S. A. *Arxivoc.* **2011**, *7*, 149.
- Pfaller, M.; Diekema, D. *Clin. Microbiol. Rev.* **2007**, *20*, 133.
- Krishnan-Natesan, S.; Chandrasekar, P. *Drugs* **2008**, *68*, 265.
- (a) Marchal, A.; Noguera, M.; Sánchez, A.; Low, J. N.; Naesens, L.; De Clercq, E.; Melguizo, M. *Eur. J. Org. Chem.* **2010**, 3823; (b) Cobo, J.; Noguera, M.; Low, J. N.; Rodríguez, R. *Tetrahedron Lett.* **2008**, *49*, 7271; (c) Marchal, A.; Melguizo, M.; Noguera, M.; Sánchez, A.; Low, J. N. *Synlett* **2002**, 255; (d) Quiroga, J.; Trilleras, J.; Insua, B.; Abonía, R.; Noguera, M.; Marchal, A.; Cobo, J. *Tetrahedron Lett.* **2008**, *49*, 3257.
- Arendrup, M.; Cuenca-Estrella, M.; Lass-Flörf, C.; Hope, W., and the Subcommittee on Antifungal Susceptibility Testing (AFST) of the ESCMID European Committee for Antimicrobial Susceptibility Testing (EUCAST), [www.eucastr.org](http://www.eucastr.org).
- CLSI, Clinical and Laboratory Standards Institute (formerly NCCLS, National Committee for Clinical and Laboratory Standards). Method M27-A3, 3rd ed.; method M-38-A2, 2nd ed.; Wayne, Ed.; NCCLS: Pennsylvania, 2008; Vol. 28 (14), pp 1–25 and Vol. 28 (16), pp 1–35.
- Bisogno, F.; Mascoti, L.; Sanchez, C.; Garibotto, F.; Giannini, F.; Kurina, M.; Enriz, R. D. *J. Agric. Food Chem.* **2007**, *55*(26), 10635.
- Poliizer, P.; Truhlar, D. G. *Chemical Applications of Atomic and Molecular Electrostatic Potentials*; Plenum Publishing: New York, 1981. 34.
- Carrupt, P. A.; El Tayar, N.; Karlén, A.; Festa, B. *Methods Enzymol.* **1991**, *202*, 638.
- Greeling, P.; Langenaeker, W.; De Proft, F.; Baeten, A. *Theoretical and Computational Chemistry.* **1996**, *3*, 587.
- Johns W.W., Finley M.T., “Handbook of Acute Toxicity of Chemicals to Fish and Aquatic Invertebrates” United States Department of the Interior Fish and Wildlife Service. Washington D.C. 1980, 1.
- Slooff, W.; De Zwart, D.; Van de Kerkhoff, J. *Aquat. Toxicol.* **1983**, *4*(2), 189.
- Frisch M.J., Trucks G.W., Schlegel H.B., Scuseria G.E., Robb M.A., Cheeseman J.R., Montgomery Jr. J.A., Vreven T., Kudin K.N., Burant J.C., Millam J.M., Iyengar S.S., Tomasi J., Barone V., Mennucci B., Cossi M., Scalmani G., Rega N., Petersson G.A., Nakatsuji H., Hada M., Ehara M., Toyota K., Fukuda R., Hasegawa J., Ishida M., Nakajima T., Honda Y., Kitao O., Nakai H., Klene M., Li X., Knox J.E., Hratchian H.P., Cross J.B., Adamo C., Jaramillo J., Gomperts R., Stratmann R.E., Yazyev O., Austin A.J., Cammi R., Pomelli C., Ochterski J.W., Ayala P.Y., Morokuma K., Voth G.A., Salvador P., Dannenberg J.J., Zakrzewski V.G., Dapprich S., Daniels A.D., Strain M.C., Farkas O., Malick D.K., Rabuck A.D., Raghavachari K., Foresman J.B., Ortiz J.V., Cui Q., Baboul A.G., Clifford S., Cioslowski J., Stefanov B.B., Liu G., Liashenko A., Piskorz P., Komaromi I., Martin R.L., Fox D.J., Keith T., Al-Laham M.A., Peng C.Y., Nanayakkara A., Challacombe M., Gill P.M.W., Johnson B., Chen W., Wong M.W., Gonzalez C., Pople J.A., Gaussian 03, Revision B.05, Gaussian, Inc., Pittsburgh, PA, 2003.
- Lee, C.; Yang, W.; Parr, R. *Phys. Rev.* **1988**, *B37*, 785.
- Miehlich, B.; Savin, A.; Stoll, H.; Preuss, M. *Chem. Phys. Lett.* **1989**, *157*, 200.
- Becke, A. *Phys. Rev. A* **1988**, *38*, 3098.
- Becke, A. *J. Chem. Phys.* **1993**, *98*, 5648.
- Flükiger P., Lüthi H.P., Portmann S., Weber J., MOLEKEL 4.0, Swiss Center for Scientific Computing, Manno, Switzerland, 2000.
- Pettersen, E. F.; Goddard, T. D.; Huang, C. C.; Couch, G. S.; Greenblatt, D. M.; Meng, E. C.; Ferrin, T. E. *J. Comput. Chem.* **2004**, *25*(13), 1605.